CALPHAD: Computer Coupling of Phase Diagrams and Thermochemistry 75 (2021) 102341

Contents lists available at ScienceDirect

Calphad

journal homepage: www.elsevier.com/locate/calphad

Recent developments for molten salt systems in Thermochimica

Max Poschmann [a], Parikshit Bajpai [b], Bernard W.N. Fitzpatrick [a], Markus H.A. Piro [a,b,*]

[a] Faculty of Energy Systems and Nuclear Science, Ontario Tech University, Oshawa, ON, Canada
[b] Faculty of Science, Ontario Tech University, Oshawa, ON, Canada

ARTICLE INFO

Keywords:
CALPHAD
Modified quasi-chemical model
Multi-physics
Thermochimica
Molten salt

ABSTRACT

The modified quasi-chemical model in the quadruplet approximation has been implemented in the open-source equilibrium thermodynamics library Thermochimica, enabling single point equilibrium calculations and sophisticated multi-physics simulations of molten salt nuclear reactor systems. Here, the derivations necessary to obtain the chemical potentials of the quadruplet species required for Gibbs energy minimization are provided. The implementation is verified via code-to-code benchmarking against FactSage. A scheme to increase computational efficiency of multi-physics simulations including Thermochimica is described and its effectiveness for molten salt systems demonstrated. Finally, a multi-physics simulation of a molten salt nuclear fuel system is presented as a demonstration problem: ORIGEN-S is used to calculate the isotopic evolution of a fuel-loaded FLiBe mixture with fission and activation products as Thermochimica predicts the phase evolution and number of moles of Cs in various phases.

1. Introduction

With the recent increase in world-wide interest in Molten Salt (nuclear) Reactor (MSR) designs [1], the need for efficient and accurate chemical thermodynamics calculations involving molten salts has grown rapidly. The MSR concept is being actively explored as a next generation nuclear reactor design in Canada, United States, Europe, and several other nation states in both large scale (e.g., approximately 1000 GWe) and small modular reactor platforms. Molten salts are also used in other engineering applications, including solar technologies. The Modified Quasi-chemical Model (MQM) [2–4] in the Quadruplet Approximation (MQMQA) [5,6] has proven to be an effective model for representing fluoride [7–12] and chloride [8,11–14] salt systems. Use of the MQMQA specifically within the FactSage [15] software in which it was first made available has been extremely popular in recent years [16–21]. Unlike other classes of thermodynamic models that focus on the mixing of constituents, the MQMQA focuses on the mixing of pairs (or quadruplets) of constituents to capture short-range ordering.

As a result of this rapidly growing interest, the MQMQA has been implemented in Thermochimica [22]. Thermochimica offers two features that distinguish it from other software: Thermochimica is a free, open-source library, and Thermochimica may be readily coupled to other software for the purposes of multi-physics simulations. In particular, Thermochimica has a history of use in multi-physics simulations of nuclear fuel materials [23–28]. Thus, implementation of MQMQA in Thermochimica enables the integration of Thermochimica into multi-physics simulations of MSRs. Due to widespread concerns over possible corrosion of MSR components by the salts themselves [29], thermochemical predictions for these systems are of particularly high importance. Through the use of Thermochimica, designers of MSR systems may be able to predict when corrosion of reactor components and formation of precipitate or gaseous species may occur, and seek combinations of chemistry and operating conditions that minimize these occurrences.

A critical step in implementing the MQMQA into Thermochimica, or any other Gibbs energy minimizer that uses explicit expressions for the chemical potentials, is the derivation of equations to represent the chemical potentials of individual species as input to the Hessian matrix. These equations have not been previously presented in the literature and are not trivial to derive. One objective of this paper is to provide a derivation of these equations, which will be helpful to others in implementing this model into their own programming. Another objective of this work is to demonstrate capabilities in using such calculations in a multi-physics code for subsequent engineering analyses.

In Section 2, the equations required to implement the MQMQA in thermodynamic software are derived. In Section 3, the implementation of these equations in Thermochimica is verified. In Section 4, a method for accelerating multi-physics simulations employing Thermochimica through re-initialization is described. In Section 5 an application of the

* Corresponding author.
E-mail address: markus.piro@ontariotechu.ca (M.H.A. Piro).

https://doi.org/10.1016/j.calphad.2021.102341
Received 30 April 2021; Received in revised form 10 August 2021; Accepted 12 August 2021
Available online 2 September 2021

MQMQA in Thermochimica to a multi-physics simulation of a molten salt nuclear fuel system is demonstrated. In Section 6 concepts for improvement and future applications are laid out.

2. Derivation of chemical potentials within the modified quasi-chemical model

Thermochimica [22] is an open-source equilibrium thermodynamics software library that solves for a unique combination of phases and concentrations that minimizes the Gibbs energy of an input system. This is performed using the Gibbs Energy Minimization (GEM) method [30]. The approach of the GEM method is to optimize the system such that the residuals in mass balance equations and the total Gibbs energy are simultaneously minimized, subject to the constraints of the Gibbs Phase Rule and conservation of mass [30,31]. Upon successful optimization of the chemical system, many thermochemical properties are available, including the mass of stable phases, the concentrations of all species in every stable solution phase, the Gibbs energy of the system, and the chemical potentials of all system components and stable species in the system. Some of these quantities may be used directly in the context of multi-physics simulations, while others might feed into parametrizations of necessary thermophysical properties.

The Gibbs energy of a solution phase depends on its composition, and a number of models and parameters have been proposed to model different phases. These models include ideal solution models, models for a single sublattice and models for multiple sublattices (e.g., Compound Energy Formalism (CEF) [32]). Despite the large number of models available to represent the Gibbs energy of a phase, the general representative expression is as follows:

$$G = G^{\circ} + G^{\mathrm{id}} + G^{\mathrm{ex}} + G^{\mathrm{phys}}, \tag{1}$$

where the Gibbs energy of the phase, G, is a sum of the reference Gibbs energy of its species, G°, which depends only on temperature, hydrostatic pressure and composition of individual species, the ideal mixing term of Gibbs energy, $G^{\mathrm{id}} = -TS^{id}$, which assumes random mixing of constituents with S^{id} denoting the entropy of mixing, and a term to account for non-ideal mixing energy, G^{ex}. The term G^{phys} captures the various physical phenomena that contribute to the Gibbs energy of the phase (e.g., magnetic contributions), and is not used within the existing MQMQA formalism.

The chemical potential of species i is by definition the partial derivative of the integral Gibbs energy of the system with respect to the number of moles of that species at constant temperature, T, and pressure, P. Mathematically, this is represented as:

$$\mu_i = \left(\frac{\partial G}{\partial n_i}\right)_{T,P,n_{j\neq i}}, \tag{2}$$

where n_i represents the number of moles of species i. One can obtain an expanded expression for chemical potential of i by substituting Eq. (1) into Eq. (2) above, which gives the following:

$$\mu_i = \underbrace{\left(\frac{\partial G^{\circ}}{\partial n_i}\right)_{T,P,n_{j\neq i}}}_{\mu_i^{\circ}} + \underbrace{\left(\frac{\partial G^{\mathrm{id}}}{\partial n_i}\right)_{T,P,n_{j\neq i}}}_{\mu_i^{\mathrm{id}}} + \underbrace{\left(\frac{\partial G^{\mathrm{ex}}}{\partial n_i}\right)_{T,P,n_{j\neq i}}}_{\mu_i^{\mathrm{ex}}}, \tag{3}$$

where the contributions to the integral Gibbs energy are obtained as the product of number of moles of a phase and the respective molar Gibbs energy contribution (i.e., $G^{\circ} = ng^{\circ}$, $G^{\mathrm{id}} = ng^{\mathrm{id}}$ and $G^{\mathrm{ex}} = ng^{\mathrm{ex}}$), with g°, g^{id} and g^{ex} denoting the molar reference Gibbs energy, the molar ideal Gibbs energy of mixing and the molar excess Gibbs energy of mixing, respectively. The partial derivative terms are referred to as the partial reference molar Gibbs energy, partial molar ideal Gibbs energy of mixing and partial molar excess Gibbs energy of mixing and are denoted by μ_i°, μ_i^{id}, and μ_i^{ex} respectively.

The MQMQA is a thermodynamic model for treating Short-Range Order (SRO) with two sublattices. The MQMQA is fundamentally different from other classes of thermodynamic models in that the focus is not on the mixing of chemical species or constituents on a lattice, but rather the mixing of species as quadruplets to capture SRO of both First-Nearest-Neighbors (FNN) and Second-Nearest-Neighbors (SNN) in liquid or solid solutions. The details of the evolution of the modified quasichemical model from pair approximation for species mixing on only one sublattice to the current quadruplet approximation on two sublattices are provided by Pelton et al. [2,3,5], Chartrand et al. [4], and Lambotte et al. [6].

2.1. Gibbs energy of modified quasichemical model phases

The integral Gibbs energy of a solution phase modeled by MQMQA can be expanded in terms of the site fractions of constituents, X_i, equivalent site fractions of constituents, Y_i, FNN pair fractions, $X_{i/k}$, SNN quadruplet fractions, $X_{ij/kl}$, and the molar quantities corresponding to these fractions. As the quadruplets are taken to be independent components of the phase, it is necessary to express all of these quantities in terms of the molar quantities of the quadruplets, $n_{ij/kl}$. In the subscript notation used throughout, a single subscript (i.e. i) indicates a cation or anion constituent, a subscript pair (i/k) indicates a pair consisting of cation constituent i and anion constituent k, and a quartet (ij/kl) indicates a quadruplet composed of cation constituents i and j, and anion constituents k and l. The quadruplet fractions are:

$$X_{ij/kl} = \frac{n_{ij/kl}}{\sum_{ab/xy} n_{ab/xy}}. \tag{4}$$

The molar quantity of a pair i/k is:

$$n_{i/k} = \sum_{ab/xy} n_{ab/xy} \frac{(\delta_{ai} + \delta_{bi})(\delta_{xk} + \delta_{yk})}{\zeta_{i/k}}, \tag{5}$$

where δ is the Kronecker delta function, and $\zeta_{i/k}$ is the FNN to SNN ratio for the pair i/k. Then, the mole fraction of a pair is:

$$X_{i/k} = \frac{n_{i/k}}{\sum_{a/x} n_{a/x}}. \tag{6}$$

Next are the site molar quantities, n_i. Since the site fractions are specific to each sublattice, the calculation of each is explicitly shown (i.e. n_i^{1st} and n_k^{2nd}). In the following discussion, the distinction will not be carried through, and the convention will be that if a constituent i is on the first sublattice, then X_i is implicitly X_i^{1st}. That said,

$$n_i^{\mathrm{1st}} = \sum_{ab/xy} n_{ab/xy} \left(\frac{\delta_{ai}}{Z^a_{ab/xy}} + \frac{\delta_{bi}}{Z^b_{ab/xy}} \right), \tag{7}$$

where $Z^i_{ij/kl}$ is the coordination number of constituent i within the quadruplet ij/kl, and

$$n_k^{\mathrm{2nd}} = \sum_{ab/xy} n_{ab/xy} \left(\frac{\delta_{xk}}{Z^x_{ab/xy}} + \frac{\delta_{yk}}{Z^y_{ab/xy}} \right). \tag{8}$$

Then, the site fractions are:

$$X_i^{\mathrm{1st}} = \frac{n_i^{\mathrm{1st}}}{\sum_a n_a^{\mathrm{1st}}}, \tag{9}$$

and

$$X_k^{\mathrm{2nd}} = \frac{n_k^{\mathrm{2nd}}}{\sum_x n_x^{\mathrm{2nd}}}. \tag{10}$$

The site-equivalent fractions (Y_i) are calculated similar to the site molar quantities (n_i), and the same convention will be used here to distinguish between sublattices. They are then:

$$Y_i^{\mathrm{1st}} = \sum_{ab/xy} X_{ab/xy} \left(\frac{\delta_{ai} + \delta_{bi}}{2} \right), \tag{11}$$

and

$$Y_k^{\mathrm{2nd}} = \sum_{ab/xy} X_{ab/xy} \left(\frac{\delta_{xk} + \delta_{yk}}{2} \right). \tag{12}$$

The coordination-equivalent fractions (F_i), which are identical to the site-equivalent fractions (Y_i) when all $\zeta_{i/k}$ are equal, are defined as [6]:

$$F_i^{\text{1st}} = \sum_{a/x} \delta_{ai} X_{a/x}, \tag{13}$$

and

$$F_k^{\text{2nd}} = \sum_{a/x} \delta_{xk} X_{a/x}. \tag{14}$$

The reference Gibbs energy term is given as follows:

$$G^\circ = \sum_{ij/kl} n_{ij/kl} g^\circ_{ij/kl}, \tag{15}$$

where $g^\circ_{ij/kl}$ denotes the reference molar Gibbs energy of the quadruplet. The configurational entropy terms can be written as the following:

$$\begin{aligned}\Delta S = -R \Bigg[&\sum_i n_i \ln(X_i) + \sum_{i/k} n_{i/k} \ln\left(\frac{X_{i/k}}{F_i F_k}\right) \\ &+ \sum_{ij/kl} n_{ij/kl} \ln\left(\frac{X_{ij/kl}}{C_{ij/kl}(X_{i/k}X_{i/l}X_{j/k}X_{j/l})^{\phi}/(Y_iY_jY_kY_l)^{\psi}}\right)\Bigg],\end{aligned} \tag{16}$$

where R is the ideal gas constant, $C_{ij/kl} = (2-\delta_{ij})(2-\delta_{kl})$ with δ being the Kronecker delta function, and the exponents ϕ and ψ take the values 1 and 1, or 3/4 and 1/2, depending on whether the original or the updated implementation of MQMQA is used [6]. The excess Gibbs energy term takes the following form:

$$\begin{aligned}G^{\text{ex}} = \frac{1}{2}\Bigg[&\sum_{ij/kl} n_{ij/kl} \Delta g_{ij/kl} \\ &+ \sum_{\substack{ij/kl \\ l=k}} \left(\frac{Z^k_{ij/kl}}{2} \sum_{\substack{m \\ m\neq k}} \frac{n_{ij/km}}{Z^k_{ij/km}}\right) \Delta g_{ij/kl} \\ &+ \sum_{\substack{ij/kl \\ j=i}} \left(\frac{Z^i_{ij/kl}}{2} \sum_{\substack{m \\ m\neq i}} \frac{n_{im/kl}}{Z^i_{im/kl}}\right) \Delta g_{ij/kl}\Bigg].\end{aligned} \tag{17}$$

In the preceding expressions, sums over i are for all constituents, sums over i/k are for all FNN pairs, and sums over ij/kl are for all FNN quadruplets. The empirical mixing parameter used to fit the Gibbs energy of formation of quadruplets, $\Delta g_{ij/kl}$, can take a variety of forms, and indeed even be composed of many of these forms. Because each $\Delta g_{ij/kl}$ contains an unknown number (possibly zero) of terms of various forms, which eventually will be summed, it is convenient to handle each of these terms independently. It should be noted that by definition for quadruplets with $i = j$ and $k = l$, the excess mixing energy is necessarily zero (as no mixing is occurring). For all other quadruplets:

$$\Delta g_{ij/kl} = \sum_{\alpha=1}^{N^{\text{ex}}_{ij/kl}} \Delta g_{ij/kl,\alpha}, \tag{18}$$

where $N^{\text{ex}}_{ij/kl}$ is the number of excess energy terms corresponding to the ij/kl quadruplet.

As described by Pelton [33], the calculation of excess mixing energy terms within the MQMQA depends on the symmetry of the ternary subsystems. These calculations are aided by the use of the variables $\xi_{ij/k}$ and $\chi_{ij/kk}$. They have been generalized to allow for the existence in the system of multiple constituents on both sublattices and to specify which of these constituents the mixing term corresponds to. $\xi_{ij/k}$ is defined as follows:

$$\xi_{ij/k} = \sum_{a=\{i,\nu\}} Y_{a/k}, \tag{19}$$

where ν represents all constituents that form asymmetrical $i-j-\nu$ ternary subsystems in which j is the asymmetric constituent. $Y_{i/k}$ is a modification of Y_i from Eq. (11) such that only contributions from quadruplets containing species k on the second sublattice are included, such that:

$$Y_{i/k} = \sum_{ab/xy} X_{ab/xy} \left(\frac{(\delta_{ai}+\delta_{bi})(\delta_{xk}+\delta_{yk})}{4}\right). \tag{20}$$

$\chi_{ij/kk}$ is defined as follows in the original implementation [5]:

$$\begin{aligned}\chi_{ij/kk} &= \frac{\sum_{a=\{i,\nu\}} \sum_{b=\{i,\nu\}} X_{ab/kk}}{\sum_{a=\{i,j,\nu,\gamma\}} \sum_{b=\{i,j,\nu,\gamma\}} X_{ab/kk}} \\ &= \frac{\sum_{a=\{i,\nu\}} \sum_{b=\{i,\nu\}} n_{ab/kk}}{\sum_{a=\{i,j,\nu,\gamma\}} \sum_{b=\{i,j,\nu,\gamma\}} n_{ab/kk}},\end{aligned} \tag{21}$$

or in the updated implementation [6,33]:

$$\begin{aligned}\chi_{ij/kk} &= \frac{\sum_{a=\{i,\nu\}} \sum_{b=\{i,\nu\}} \sum_x \sum_y \frac{\delta_{kx}+\delta_{ky}}{2} X_{ab/xy}}{\sum_{a=\{i,j,\nu,\gamma\}} \sum_{b=\{i,j,\nu,\gamma\}} \sum_x \sum_y \frac{\delta_{kx}+\delta_{ky}}{2} X_{ab/xy}} \\ &= \frac{\sum_{a=\{i,\nu\}} \sum_{b=\{i,\nu\}} \sum_x \sum_y \frac{\delta_{kx}+\delta_{ky}}{2} n_{ab/xy}}{\sum_{a=\{i,j,\nu,\gamma\}} \sum_{b=\{i,j,\nu,\gamma\}} \sum_x \sum_y \frac{\delta_{kx}+\delta_{ky}}{2} n_{ab/xy}},\end{aligned} \tag{22}$$

where γ represents all constituents that form asymmetrical $i-j-\gamma$ ternary subsystems in which i is the asymmetric constituent. The sums over x and y are for all constituents on the second sublattice. These equations can be reversed to apply to the second sublattice, but for the sake of brevity from here on only mixing on the first sublattice will be shown explicitly. In Eq. (21), it can be observed that because the numerator and denominator involve the same powers of $X_{ij/kl}$, the mole fractions can be replaced with the molar quantities.

There are numerous possibilities for the form of each $\Delta g_{ij/kl,\alpha}$. These include binary mixing terms proportional to the quadruplet fractions:

$$\Delta g_{ij/kk,\alpha} = g_{ij/kk,\alpha} \cdot \chi^{p_\alpha}_{ij/kk} \chi^{q_\alpha}_{ji/kk}, \tag{23}$$

binary mixing proportional to equivalent site fractions:

$$\Delta g_{ij/kk,\alpha} = g_{ij/kk,\alpha} \cdot \frac{\xi^{p_\alpha}_{ij/k} \xi^{q_\alpha}_{ji/k}}{(\xi_{ij/k}+\xi_{ji/k})^{p_\alpha+q_\alpha}}, \tag{24}$$

ternary mixing proportional to the quadruplet fractions:

$$\Delta g_{ij(m)/kk,\alpha} = g_{ij(m)/kk,\alpha} \cdot \chi^{p_\alpha}_{ij/kk} \chi^{q_\alpha}_{ji/kk} \cdot \begin{cases} \left(\frac{Y_{m/k}}{\xi_{ji/k}}\right)\left(1-\frac{Y_{j/k}}{\xi_{ji/k}}\right)^{r_\alpha-1} & m \in \gamma \\ \left(\frac{Y_{m/k}}{\xi_{ij/k}}\right)\left(1-\frac{Y_{i/k}}{\xi_{ij/k}}\right)^{r_\alpha-1} & m \in \nu \\ Y_{m/k}\left(1-\xi_{ij/k}-\xi_{ji/k}\right)^{r_\alpha-1} & m \notin \{\nu,\gamma\}, \end{cases} \tag{25}$$

and ternary mixing proportional to equivalent site fractions:

$$\begin{aligned}\Delta g_{ij(m)/kk,\alpha} = g_{ij(m)/kk,\alpha} \cdot \frac{\xi^{p_\alpha}_{ij/k} \xi^{q_\alpha}_{ji/k}}{(\xi_{ij/k}+\xi_{ji/k})^{p_\alpha+q_\alpha}} \\ \cdot \begin{cases} \left(\frac{Y_{m/k}}{\xi_{ji/k}}\right)\left(1-\frac{Y_{j/k}}{\xi_{ji/k}}\right)^{r_\alpha-1} & m \in \gamma \\ \left(\frac{Y_{m/k}}{\xi_{ij/k}}\right)\left(1-\frac{Y_{i/k}}{\xi_{ij/k}}\right)^{r_\alpha-1} & m \in \nu \\ Y_{m/k}\left(1-\xi_{ij/k}-\xi_{ji/k}\right)^{r_\alpha-1} & m \notin \{\nu,\gamma\}, \end{cases}\end{aligned} \tag{26}$$

where in the above equations p_α, q_α, and r_α are integer exponents chosen for the excess mixing term α.

In the types of mixing terms described in Eqs. (23)–(26), there is a restriction of having only one constituent involved on either the first or second sublattice. Expressions for mixing on the first sublattice are shown. Note that the terms preceding the cases in Eqs. (25) and (26) correspond to Eqs. (23) and (24), and that the terms within the cases are identical for the two forms of ternary mixing. The cases $m \in \gamma$, $m \in \nu$, and $m \notin \{\nu,\gamma\}$ correspond to the ternary system $i-j-m$ being

asymmetric with i as the asymmetric constituent, asymmetric with j as the asymmetric constituent, and either asymmetric with m as the asymmetric constituent or symmetric, respectively. m cannot be equal to either of i and j, as this would not indicate a ternary subsystem.

2.2. Derivation of chemical potential equations

In the MQMQA, the chemical potentials are defined as partial derivatives in terms of the molar quantities of the various quadruplets (analogous to the compound end members in the CEF). Following the procedure employed to compute the Gibbs energies, the chemical potentials are computed as sums of derivatives of the various energetic contributions:

$$\begin{aligned}\mu_{ij/kl} &= \left(\frac{\partial G}{\partial n_{ij/kl}}\right)_{T,P,n_{(ab/xy)\neq(ij/kl)}} \\ &= \left(\frac{\partial G^{\circ}}{\partial n_{ij/kl}} - T\frac{\partial \Delta S}{\partial n_{ij/kl}} + \frac{\partial G^{\mathrm{ex}}}{\partial n_{ij/kl}}\right)_{T,P,n_{(ab/xy)\neq(ij/kl)}}.\end{aligned} \tag{27}$$

The following sub-sections will derive each of the terms in Eq. (27).

2.2.1. Derivation of the reference Gibbs energy and entropic contributions to chemical potential equations

The partial molar reference Gibbs energy is defined as follows:

$$\frac{\partial G^{\circ}}{\partial n_{ij/kl}} = g^{\circ}_{ij/kl}. \tag{28}$$

The entropic contributions to chemical potentials are greatly simplified by the cancellation of the derivatives of the terms within logarithms, which results in:

$$\begin{aligned}\frac{\partial \Delta S}{\partial n_{ij/kl}} = R\Bigg[&\sum_m \frac{\partial n_m}{\partial n_{ij/kl}}\ln(X_m) + \sum_{m/z}\frac{\partial n_{m/z}}{\partial n_{ij/kl}}\ln\left(\frac{X_{m/z}}{F_m F_z}\right) \\ &+\ln\left(\frac{X_{ij/kl}}{C_{ij/kl}(X_{i/k}X_{i/l}X_{j/k}X_{j/l})^{\phi}/(Y_iY_jY_kY_l)^{\psi}}\right)\Bigg],\end{aligned} \tag{29}$$

where the sum over m is over all constituents, and the sum over m/z is over all pairs. This leaves only the values of the partial derivatives $\frac{\partial n_m}{\partial n_{ij/kl}}$ and $\frac{\partial n_{m/z}}{\partial n_{ij/kl}}$ to be determined as follows:

$$\frac{\partial n_m}{\partial n_{ij/kl}} = \frac{\delta_{im}}{Z^i_{ij/kl}} + \frac{\delta_{jm}}{Z^j_{ij/kl}} + \frac{\delta_{km}}{Z^k_{ij/kl}} + \frac{\delta_{lm}}{Z^l_{ij/kl}}. \tag{30}$$

While the previous expression is general, it is worth noting that m can never be equal to i or j and k or l at the same time, as the constituent is on either the first sublattice or the second. Finally,

$$\frac{\partial n_{m/z}}{\partial n_{ij/kl}} = \frac{(\delta_{im}+\delta_{jm})(\delta_{kz}+\delta_{lz})}{\zeta_{m/z}}, \tag{31}$$

where $\zeta_{m/z}$ is the ratio of FNN to SNN for the FNN pair m/z.

2.2.2. Derivation of the partial molar excess Gibbs energy contribution to chemical potential

Due to the dependence of excess mixing Gibbs energy terms on the mole fractions of phase components, the derivative of each term with respect to molar amounts of all quadruplets are non-zero, unless if all exponents are zero. This results in many cases for the derivatives, as within each form there are cases for the quadruplets explicitly involved in the mixing, and for the rest that are implicitly involved. Fortunately, as will be shown, these derivatives can be written compactly in terms of the excess mixing energies themselves. It is crucial not to forget the product rule resulting from Eq. (17), in which molar quantities are multiplied by the sums of individual excess mixing terms:

$$\begin{aligned}\frac{\partial G^{\mathrm{ex}}}{\partial n_{ab/xy}} = \frac{1}{2}\Bigg[&\sum_{ij/kl}\left\{\frac{\partial n_{ij/kl}}{\partial n_{ab/xy}}\Delta g_{ij/kl} + n_{ij/kl}\frac{\partial \Delta g_{ij/kl}}{\partial n_{ab/xy}}\right\} \\ &+\sum_{\substack{ij/kl\\ l=k}}\left\{\left(\frac{Z^k_{ij/kl}}{2}\sum_{\substack{m\\ m\neq k}}\frac{\frac{\partial n_{ij/km}}{\partial n_{ab/xy}}}{Z^k_{ij/km}}\right)\Delta g_{ij/kl}\right. \\ &\left.+\left(\frac{Z^k_{ij/kl}}{2}\sum_{\substack{m\\ m\neq k}}\frac{n_{ij/km}}{Z^k_{ij/km}}\right)\frac{\partial \Delta g_{ij/kl}}{\partial n_{ab/xy}}\right\} \\ &+\sum_{\substack{ij/kl\\ j=i}}\left\{\left(\frac{Z^i_{ij/kl}}{2}\sum_{\substack{m\\ m\neq i}}\frac{\frac{\partial n_{im/kl}}{\partial n_{ab/xy}}}{Z^i_{im/kl}}\right)\Delta g_{ij/kl}\right. \\ &\left.+\left(\frac{Z^i_{ij/kl}}{2}\sum_{\substack{m\\ m\neq i}}\frac{n_{im/kl}}{Z^i_{im/kl}}\right)\frac{\partial \Delta g_{ij/kl}}{\partial n_{ab/xy}}\right\}\Bigg].\end{aligned} \tag{32}$$

$\frac{\partial n_{ij/kl}}{\partial n_{ab/xy}}$ is equal to 1 if $i=a$, $j=b$, $k=x$, and $l=y$, and is 0 otherwise. Thus, the foregoing expression simplifies to the following:

$$\begin{aligned}\frac{\partial G^{\mathrm{ex}}}{\partial n_{ab/xy}} = \frac{1}{2}\Bigg[&\Delta g_{ab/xy} + \sum_{ij/kl}\left\{n_{ij/kl}\frac{\partial \Delta g_{ij/kl}}{\partial n_{ab/xy}}\right\} \\ &+\left(\frac{Z^x_{ab/xx}}{2Z^x_{ab/xy}} + \frac{Z^y_{ab/yy}}{2Z^y_{ab/xy}}\right)\Delta g_{ab/xy} \\ &+\sum_{\substack{ij/kl\\ l=k}}\left\{\left(\frac{Z^k_{ij/kl}}{2}\sum_{\substack{m\\ m\neq k}}\frac{n_{ij/km}}{Z^k_{ij/km}}\right)\frac{\partial \Delta g_{ij/kl}}{\partial n_{ab/xy}}\right\} \\ &+\left(\frac{Z^a_{aa/xy}}{2Z^a_{ab/xy}} + \frac{Z^b_{bb/xy}}{2Z^b_{ab/xy}}\right)\Delta g_{ab/xy} \\ &+\sum_{\substack{ij/kl\\ j=i}}\left\{\left(\frac{Z^i_{ij/kl}}{2}\sum_{\substack{m\\ m\neq i}}\frac{n_{im/kl}}{Z^i_{im/kl}}\right)\frac{\partial \Delta g_{ij/kl}}{\partial n_{ab/xy}}\right\}\Bigg].\end{aligned} \tag{33}$$

By substituting Eq. (18) into Eq. (33), $\Delta g_{ij/kl}$ can be replaced by $\sum_{\alpha=1}^{N^{\mathrm{ex}}_{ij/kl}}\Delta g_{ij/kl,\alpha}$. Thus, in all cases, the quantity of interest remains $\frac{\partial \Delta g_{ij/kl,\alpha}}{\partial n_{ab/xy}}$. The possible forms for $\Delta g_{ij/kl,\alpha}$ will be approached in the same order as before. Starting with binary mixing based on quadruplet fractions:

$$\begin{aligned}\frac{\partial(\Delta g_{ij/kk,\alpha})}{\partial n_{ab/xy}} = &\frac{\Delta g_{ij/kk,\alpha}}{\sum_{cd/vw} n_{cd/vw}}\cdot\frac{\delta_{xk}\delta_{yk}}{\sum_{c=\{i,j,v,\gamma\}}\sum_{d=\{i,j,v,\gamma\}} X_{cd/kk}} \\ &\times\Bigg[\frac{\left(\sum_{e=i,v}\delta_{ae}\right)\left(\sum_{e=i,v}\delta_{be}\right)p_{\alpha}}{\chi_{ij/kk}} \\ &+\frac{\left(\sum_{e=j,\gamma}\delta_{ae}\right)\left(\sum_{e=j,\gamma}\delta_{be}\right)q_{\alpha}}{\chi_{ji/kk}} \\ &-\left(\sum_{e=i,v}\delta_{ae}+\sum_{e=j,\gamma}\delta_{ae}\right)\left(\sum_{e=i,v}\delta_{be}+\sum_{e=j,\gamma}\delta_{be}\right) \\ &\times\left(p_{\alpha}+q_{\alpha}\right)\Bigg].\end{aligned} \tag{34}$$

In these equations, advantage has been taken of the equal powers of the mole fractions $X_{ij/kl}$ terms in the numerator and denominator to transform these to the molar quantities $n_{ij/kl}$ prior to differentiation.

Eq. (34) is convenient for computational purposes because the derivative of the excess energy term can be expressed relatively compactly in terms of the excess energy term itself. Furthermore, all quantities can be written in terms of $X_{ij/kl}$ except the denominator of the leading fraction, which will cancel with a similar term in Eq. (33).

Next, one can apply the same procedure to binary mixing based on equivalent site fractions:

$$\begin{aligned}\frac{\partial(\Delta g_{ij/kk,\alpha})}{\partial n_{ab/xy}} = \frac{\Delta g_{ij/kk,\alpha}}{\sum_{cd/vw} n_{cd/vw}} \Bigg[\left(\sum_{e=\{i,\nu\}} \frac{(\delta_{ae}+\delta_{be})(\delta_{xk}+\delta_{yk})}{4} \right) \\ \times \left(\frac{p_\alpha}{\xi_{ij/k}} - \frac{p_\alpha + q_\alpha}{\xi_{ij/k}+\xi_{ji/k}} \right) \\ + \left(\sum_{e=\{j,\gamma\}} \frac{(\delta_{ae}+\delta_{be})(\delta_{xk}+\delta_{yk})}{4} \right) \\ \times \left(\frac{q_\alpha}{\xi_{ji/k}} - \frac{p_\alpha + q_\alpha}{\xi_{ij/k}+\xi_{ji/k}} \right) \Bigg],\end{aligned} \tag{35}$$

which has similar properties to Eq. (34).

As shown in Eqs. (25) and (26), the ternary mixing terms include three possible cases. To compute the derivatives of Eqs. (25) and (26), one must first differentiate these three cases. First, the case in which $m \in \gamma$ results in:

$$\begin{aligned}&\frac{\partial}{\partial n_{ab/xy}} \left[\left(\frac{Y_{m/k}}{\xi_{ji/k}} \right) \left(1 - \frac{Y_{j/k}}{\xi_{ji/k}} \right)^{r_\alpha - 1} \right] \\ &= \left(\frac{1}{\sum_{cd/vw} n_{cd/vw}} \right) \left(\frac{Y_{m/k}}{\xi_{ji/k}} \right) \left(1 - \frac{Y_{j/k}}{\xi_{ji/k}} \right)^{r_\alpha - 1} \\ &\quad \cdot \left[\left(\frac{(\delta_{am}+\delta_{bm})(\delta_{xk}+\delta_{yk})}{4 Y_{m/k}} \right) - \left(\sum_{e=\{j,\gamma\}} \frac{(\delta_{ae}+\delta_{be})(\delta_{xk}+\delta_{yk})}{4\xi_{ji/k}} \right) \right. \\ &\quad - \left(\frac{r_\alpha - 1}{\xi_{ji/k}} \right) \left(1 - \frac{Y_{j/k}}{\xi_{ji/k}} \right)^{-1} \left\{ \left(\frac{(\delta_{aj}+\delta_{bj})(\delta_{xk}+\delta_{yk})}{4} \right) \right. \\ &\quad \left. \left. - Y_{j/k} \left(\sum_{e=\{j,\gamma\}} \frac{(\delta_{ae}+\delta_{be})(\delta_{xk}+\delta_{yk})}{4\xi_{ji/k}} \right) \right\} \right]\end{aligned} \tag{36}$$

Similarly, the case in which $m \in \nu$ results in:

$$\begin{aligned}&\frac{\partial}{\partial n_{ab/xy}} \left[\left(\frac{Y_{m/k}}{\xi_{ij/k}} \right) \left(1 - \frac{Y_{i/k}}{\xi_{ij/k}} \right)^{r_\alpha - 1} \right] \\ &= \left(\frac{1}{\sum_{cd/vw} n_{cd/vw}} \right) \left(\frac{Y_{m/k}}{\xi_{ij/k}} \right) \left(1 - \frac{Y_{i/k}}{\xi_{ij/k}} \right)^{r_\alpha - 1} \\ &\quad \cdot \left[\left(\frac{(\delta_{am}+\delta_{bm})(\delta_{xk}+\delta_{yk})}{4 Y_{m/k}} \right) - \left(\sum_{e=\{i,\nu\}} \frac{(\delta_{ae}+\delta_{be})(\delta_{xk}+\delta_{yk})}{4\xi_{ij/k}} \right) \right. \\ &\quad - \left(\frac{r_\alpha - 1}{\xi_{ij/k}} \right) \left(1 - \frac{Y_{i/k}}{\xi_{ij/k}} \right)^{-1} \left\{ \left(\frac{(\delta_{ai}+\delta_{bi})(\delta_{xk}+\delta_{yk})}{4} \right) \right. \\ &\quad \left. \left. - Y_{i/k} \left(\sum_{e=\{i,\nu\}} \frac{(\delta_{ae}+\delta_{be})(\delta_{xk}+\delta_{yk})}{4\xi_{ij/k}} \right) \right\} \right]\end{aligned} \tag{37}$$

The case in which $m \notin \{\nu, \gamma\}$ results in:

$$\begin{aligned}\frac{\partial}{\partial n_{ab/xy}} \left[Y_{m/k} \left(1 - \xi_{ij/k} - \xi_{ji/k} \right)^{r_\alpha - 1} \right] = \left(\frac{Y_{m/k} \left(1 - \xi_{ij/k} - \xi_{ji/k} \right)^{r_\alpha - 1}}{\sum_{cd/vw} n_{cd/vw}} \right) \\ \cdot \left[-(r_\alpha) + \left(\frac{(\delta_{am}+\delta_{bm})(\delta_{xk}+\delta_{yk})}{4} \right) \left(\frac{1}{Y_{m/k}} \right) \right. \\ + (r_\alpha - 1) \left\{ 1 - \xi_{ij} - \xi_{ji} \right\}^{-1} \\ \cdot \left\{ 1 - \sum_{e=\{i,\nu\}} \left(\frac{(\delta_{ae}+\delta_{be})(\delta_{xk}+\delta_{yk})}{4} \right) \right. \\ \left. \left. - \sum_{e=\{j,\gamma\}} \left(\frac{(\delta_{ae}+\delta_{be})(\delta_{xk}+\delta_{yk})}{4} \right) \right\} \right]\end{aligned} \tag{38}$$

With all the necessary pieces in place, the derivatives for ternary excess energy terms can be formed by combining Eqs. (36), (37), and (38) with Eq. (34) (for the quadruplet fraction formulation) and with Eq. (35) (for the site fraction formulation). Taking the quadruplet fraction case first: Eq. (37) is given in Box I where the cases in the last term were described below equation (26). In the second line of Eq. (39), the term $\delta_{xk}\delta_{yk}$ is replaced with $\frac{1}{2}(\delta_{xk}+\delta_{yk})$ for the updated implementation of MQMQA [6,33]. Finally, the site fraction case: Eq. (38) is given in Box II.

The equations presented here are in a form suitable for direct implementation into software, and have been incorporated in Thermochimica in as similar a manner as is possible within the Fortran language. This is intended to enhance readability of the Thermochimica source code to enable verification, modification, use, and comparison with other software in which the MQMQA is implemented. In the following sections, we will demonstrate verification, modification, and use of the MQMQA in Thermochimica.

3. Implementation of the modified quasi-chemical model in Thermochimica

To verify the accuracy of calculations performed using modified routines in Thermochimica, direct benchmarking comparisons were made with the commercial software FactSage [15], using the molten salt thermodynamic database (MSTDB) [34]. These calculations sample different regions of the MSTDB phase space, namely a pure molten salt, a molten salt and solid precipitate mixture, a molten salt and gas phase mixture, a very simple pure molten salt case including only F and U, and complex nuclear fuel salt mixtures with compositions given in Tables 1 and 2. Each test compares Thermochimica output to data calculated by FactSage, and thus if these tests pass it is confirmed that Thermochimica is performing correctly for these representative conditions. A successful benchmark is taken to be one where the relative difference between the mole fraction of a solution species is within 0.1%. The results from the final two test cases are displayed in Fig. 1 to show the agreement between Thermochimica and FactSage. The MSTDB chloride database includes vacancies as a possible constituent on the anion sublattice, and thus this test includes reciprocal quadruplets of the form AB/XY.

It is worth noting that under certain conditions the Hessian matrix corresponding to a molten salt system described by the MQMQA can be under-determined, as detailed by Piro et al. [35]. This is not the case when multiple constituents corresponding to different valence states of the same element (for example, U^{3+} and U^{4+} in the MSTDB) are present in the system. Further work is required to develop an elegant and general solution to address this issue within Thermochimica.

$$\frac{\partial \Delta g_{ij(m)/kk,\alpha}}{\partial n_{ab/xy}} = \frac{\Delta g_{ij(m)/kk,\alpha}}{\sum_{cd/vw} n_{cd/vw}}$$

$$\cdot \left[\frac{\delta_{xk}\delta_{yk}}{\sum_{c=\{i,j,\nu,\gamma\}} \sum_{d=\{i,j,\nu,\gamma\}} X_{cd/kk}} \left[\frac{\left(\sum_{e=i,\nu} \delta_{ae}\right)\left(\sum_{e=i,\nu} \delta_{be}\right) p_\alpha}{\chi_{ij/kk}} + \frac{\left(\sum_{e=ij,\gamma} \delta_{ae}\right)\left(\sum_{e=j,\gamma} \delta_{be}\right) q_\alpha}{\chi_{ji/kk}} \right.\right.$$

$$\left.\left. - \left(\left(\sum_{e=i,\nu} \delta_{ae}\right) + \left(\sum_{e=ij,\gamma} \delta_{ae}\right)\right)\left(\left(\sum_{e=i,\nu} \delta_{be}\right) + \left(\sum_{e=j,\gamma} \delta_{be}\right)\right)\left(p_\alpha + q_\alpha\right) \right] \right.$$

$$+ \left\{ \begin{array}{ll} \left(\frac{(\delta_{am}+\delta_{bm})(\delta_{xk}+\delta_{yk})}{4Y_{m/k}}\right) - \left(\sum_{e=\{j,\gamma\}} \frac{(\delta_{ae}+\delta_{be})(\delta_{xk}+\delta_{yk})}{4\xi_{ji/k}}\right) & \\ - \left(\frac{r_\alpha - 1}{\xi_{ji/k}}\right)\left(1 - \frac{Y_{j/k}}{\xi_{ji/k}}\right)^{-1} \left\{ \left(\frac{(\delta_{aj}+\delta_{bj})(\delta_{xk}+\delta_{yk})}{4}\right) - Y_{j/k}\left(\sum_{e=\{j,\gamma\}} \frac{(\delta_{ae}+\delta_{be})(\delta_{xk}+\delta_{yk})}{4\xi_{ji/k}}\right)\right\} & m \in \gamma \\ \left(\frac{(\delta_{am}+\delta_{bm})(\delta_{xk}+\delta_{yk})}{4Y_{m/k}}\right) - \left(\sum_{e=\{i,\nu\}} \frac{(\delta_{ae}+\delta_{be})(\delta_{xk}+\delta_{yk})}{4\xi_{ij/k}}\right) & \\ - \left(\frac{r_\alpha - 1}{\xi_{ij/k}}\right)\left(1 - \frac{Y_{i/k}}{\xi_{ij/k}}\right)^{-1} \left\{ \left(\frac{(\delta_{ai}+\delta_{bi})(\delta_{xk}+\delta_{yk})}{4}\right) - Y_{i/k}\left(\sum_{e=\{i,\nu\}} \frac{(\delta_{ae}+\delta_{be})(\delta_{xk}+\delta_{yk})}{4\xi_{ij/k}}\right)\right\} & m \in \nu \\ -(r_\alpha) + \left(\frac{(\delta_{am}+\delta_{bm})(\delta_{xk}+\delta_{yk})}{4}\right)\left(\frac{1}{Y_{m/k}}\right) + (r_\alpha - 1)\left\{1 - \xi_{ij} - \xi_{ji}\right\}^{-1} & \\ \quad \cdot \left\{1 - \sum_{e=\{i,\nu\}} \left(\frac{(\delta_{ae}+\delta_{be})(\delta_{xk}+\delta_{yk})}{4}\right) - \sum_{e=\{j,\gamma\}} \left(\frac{(\delta_{ae}+\delta_{be})(\delta_{xk}+\delta_{yk})}{4}\right)\right\} & m \notin \{\nu,\gamma\} \end{array} \right\}, \tag{39}$$

Box I.

$$\frac{\partial \Delta g_{ij(m)/kk,\alpha}}{\partial n_{ab/xy}} = \frac{\Delta g_{ij(m)/kk,\alpha}}{\sum_{cd/vw} n_{cd/vw}}$$

$$\cdot \left[\left(\sum_{e=\{i,\nu\}} \frac{(\delta_{ae}+\delta_{be})(\delta_{xk}+\delta_{yk})}{4} \right)\left(\frac{p_\alpha}{\xi_{ij/k}} - \frac{p_\alpha + q_\alpha}{\xi_{ij/k} + \xi_{ji/k}}\right) \right.$$

$$\left. + \left(\sum_{e=\{j,\gamma\}} \frac{(\delta_{ae}+\delta_{be})(\delta_{xk}+\delta_{yk})}{4} \right)\left(\frac{q_\alpha}{\xi_{ji/k}} - \frac{p_\alpha + q_\alpha}{\xi_{ij/k} + \xi_{ji/k}}\right) \right.$$

$$+ \left\{ \begin{array}{ll} \left(\frac{(\delta_{am}+\delta_{bm})(\delta_{xk}+\delta_{yk})}{4Y_{m/k}}\right) - \left(\sum_{e=\{j,\gamma\}} \frac{(\delta_{ae}+\delta_{be})(\delta_{xk}+\delta_{yk})}{4\xi_{ji/k}}\right) & \\ - \left(\frac{r_\alpha - 1}{\xi_{ji/k}}\right)\left(1 - \frac{Y_{j/k}}{\xi_{ji/k}}\right)^{-1} \left\{ \left(\frac{(\delta_{aj}+\delta_{bj})(\delta_{xk}+\delta_{yk})}{4}\right) - Y_{j/k}\left(\sum_{e=\{j,\gamma\}} \frac{(\delta_{ae}+\delta_{be})(\delta_{xk}+\delta_{yk})}{4\xi_{ji/k}}\right)\right\} & m \in \gamma \\ \left(\frac{(\delta_{am}+\delta_{bm})(\delta_{xk}+\delta_{yk})}{4Y_{m/k}}\right) - \left(\sum_{e=\{i,\nu\}} \frac{(\delta_{ae}+\delta_{be})(\delta_{xk}+\delta_{yk})}{4\xi_{ij/k}}\right) & \\ - \left(\frac{r_\alpha - 1}{\xi_{ij/k}}\right)\left(1 - \frac{Y_{i/k}}{\xi_{ij/k}}\right)^{-1} \left\{ \left(\frac{(\delta_{ai}+\delta_{bi})(\delta_{xk}+\delta_{yk})}{4}\right) - Y_{i/k}\left(\sum_{e=\{i,\nu\}} \frac{(\delta_{ae}+\delta_{be})(\delta_{xk}+\delta_{yk})}{4\xi_{ij/k}}\right)\right\} & m \in \nu \\ -(r_\alpha) + \left(\frac{(\delta_{am}+\delta_{bm})(\delta_{xk}+\delta_{yk})}{4}\right)\left(\frac{1}{Y_{m/k}}\right) + (r_\alpha - 1)\left\{1 - \xi_{ij} - \xi_{ji}\right\}^{-1} & \\ \quad \cdot \left\{1 - \sum_{e=\{i,\nu\}} \left(\frac{(\delta_{ae}+\delta_{be})(\delta_{xk}+\delta_{yk})}{4}\right) - \sum_{e=\{j,\gamma\}} \left(\frac{(\delta_{ae}+\delta_{be})(\delta_{xk}+\delta_{yk})}{4}\right)\right\} & m \notin \{\nu,\gamma\} \end{array} \right\}. \tag{40}$$

Box II.

4. Performance enhancement through re-initialization

In a stand-alone Thermochimica calculation, the leveling algorithm [36,37] is used to provide an initial estimation of the phase assemblage and the element potentials. The leveling method is a first approximation to equilibrium, which does not include mixing between species in a solution phase — all species and phases are temporarily treated as stoichiometric phases. Once this initial estimate of the

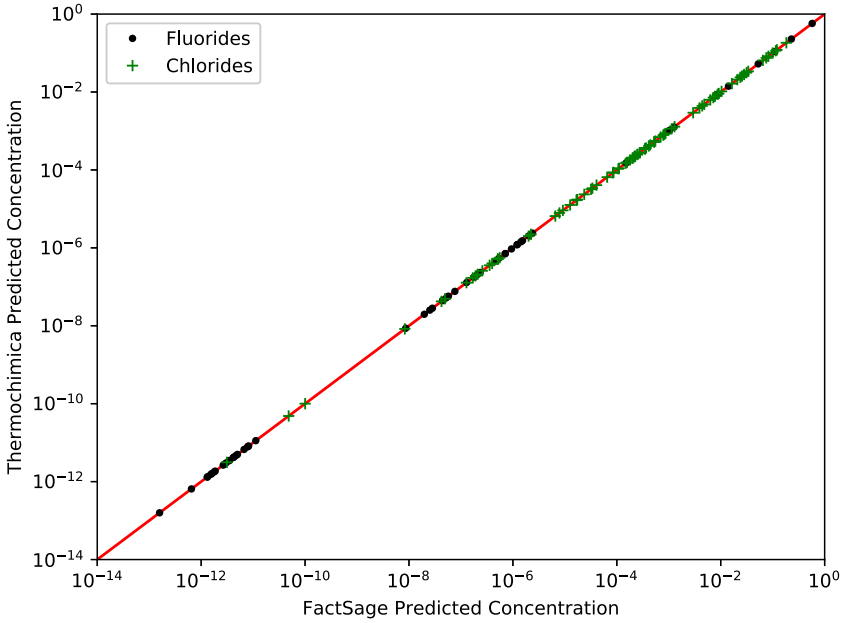

Fig. 1. Output species concentrations predictions from Thermochimica and FactSage for the nuclear fuel salt mixtures with compositions given in Tables 1 and 2 at 1500 K and 1 atm. Both codes predict the only stable phase to be the MQMQA liquid phase, and report integral Gibbs energies of −2.97876E+11 J for the fluoride case and −3.68872E+11 J for the chloride case. The red line indicates perfect agreement.

Table 1
Composition of fluoride-based nuclear fuel salt mixture used for code verification.

Element	Mass [moles]
Pu	1.9780×10^{-1}
U	9.9695×10^{3}
Nd	3.3553×10^{-1}
Ce	4.2081×10^{-1}
La	1.4912×10^{-1}
Cs	4.2326×10^{-1}
Rb	8.1960×10^{-2}
F	4.4000×10^{5}
Be	1.0000×10^{5}
Li	2.0216×10^{5}

Table 2
Composition of chloride-based nuclear fuel salt mixture used for code verification.

Element	Mass [moles]
Pu	2×10^{3}
U	4×10^{3}
Cs	4×10^{2}
K	2×10^{5}
Cl	6×10^{5}
Mg	1×10^{5}
Na	2×10^{5}
Li	1×10^{5}

phase assemblage has been obtained, the GEM method [30] is used to determine the combination of phases and phase compositions that yields the lowest integral Gibbs energy. This is done by iteratively manipulating the quantities of species to minimize the integral Gibbs energy, adding to the assemblage those phases with a negative driving force, and removing phases from the assemblage that tend to form negative (i.e., non-physical) quantities.

In a new re-initialization method [38], the first Thermochimica calculation proceeds as above. However, immediately after each calculation, key chemical information provided by Thermochimica is stored (i.e. by MOOSE [39] at each node in the finite-element method mesh). Then, on following calls to Thermochimica, that information is reused to provide an enhanced estimation of the initial phase assemblage and species concentrations. This has two positive effects: the leveling solver may be bypassed, and (more significantly) the resulting assemblage and concentrations are typically much closer to the equilibrium state than those provided by the leveling solver. When the GEM solver begins with a better initial estimate, it takes many fewer steps to converge and calculation time is greatly decreased. Of course, storage of this initialization data at each node or integration point results in increased total memory usage as well as additional memory operations; however, benchmark tests demonstrate that these costs are greatly outweighed by the reduced number of calculation cycles.

The re-initialization method has been used in conjunction with a variety of chemical systems. In particular, performance benchmarking was conducted using four systems of varying complexity: (1) a simple system containing only C and O; (2) a UO_2 nuclear fuel system (representative of light water reactor or CANDU fuel) containing U, Nd, Ce, La, Ba, Cs, Pd, Rh, Ru, Mo, Zr, Sr, and O; (3) the same nuclear fuel system with the following additional elements included: Pu, Np, Pr, Xe, I, Te, Tc, Y, Rb, and H; and (4) a FLiBe nuclear fuel salt system including U, F, and fission products Nd, Ce, La, Cs, Rb, and Ca. For each system, calculation series with constant conditions, varying temperature, and varying compositions were conducted. The speedup provided by the re-initialization algorithm was measured for each case and the results are shown in Fig. 2. For the simple C–O system (i.e., Case #1), speedup was small because re-initialization overhead competes with the reduction of GEM iterations, but for the most chemically complex fission product system (i.e., Case # 3), speedup above 10× in terms of wall-clock time was observed. This scheme is particularly effective for the FLiBe-based fuel salt example system, likely due to the large number of chemical species required to represent salt phases in MQM.

Performance of coupled code systems has been improved substantially by the use of this method, allowing for greater numbers of finite elements and time steps to be used in conjunction with equilibrium thermochemical calculations.

5. Applications to multi-physics simulations of nuclear fuels

Thermochimica has been coupled with ORIGEN-S [41], which is an isotopic evolution code that performs nuclear depletion, decay,

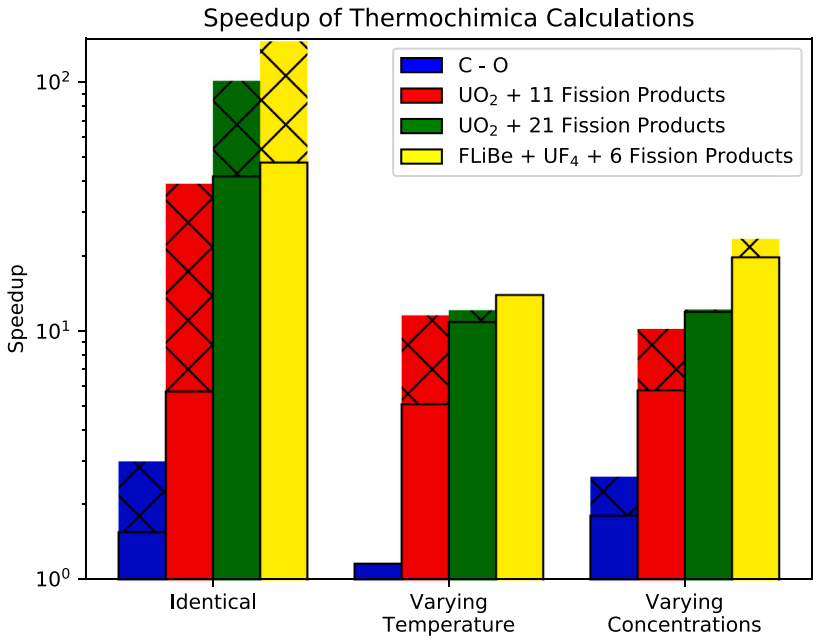

Fig. 2. Speedup due to use of the re-initialization method for stand-alone Thermochimica calculations of (1) the carbon–oxygen, (2) uranium dioxide with 11 fission products, (3) uranium dioxide with 21 fission products, and (4) FLiBe with UF_4 and 6 fission products. The solid portions of the bars indicate speedup as measured by wall-clock time, which the hatched portions indicate the speedup as measured by number of GEM iterations. The latter is greater in all cases except the C–O and FLiBe systems under varying temperatures.

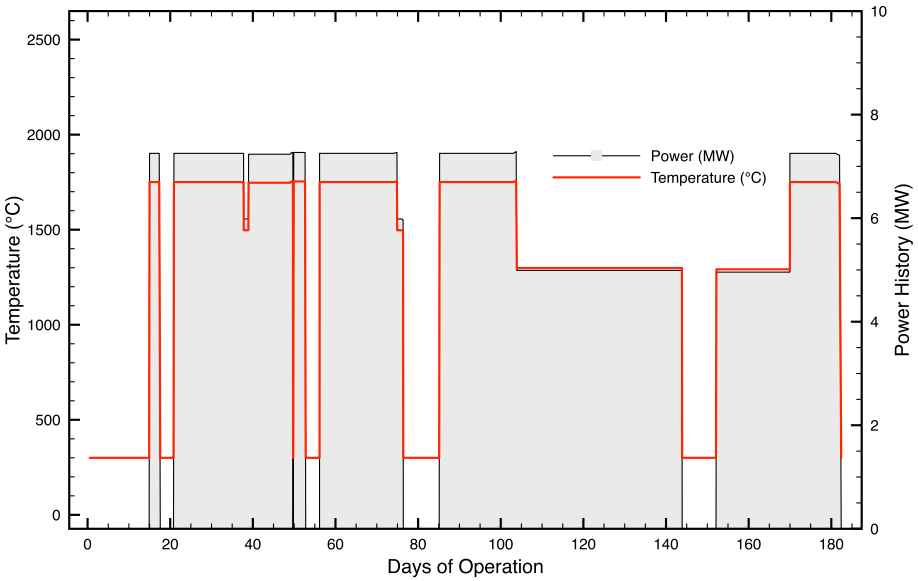

Fig. 3. Power history from the MSRE [40] and temperature of fuel mixture, simulated by a linear function of the power.

and transmutation calculations. In this example calculation, a FLiBe mixture loaded with UF_4 is subjected to irradiation using a sample power history of the Molten Salt Reactor Experiment (MSRE) reactor at the Oak Ridge National Laboratory (ORNL) in the 1960s [40]. This power history controls both the temperature of the salt mixture (simulated from a linear function of the power) and the isotopic evolution. Initially, the temperature function was based on the actual MSRE operating temperatures reported by ORNL; however, this produced only one liquid solution phase. In this implementation, the temperature range has been expanded so that ideal gas, liquid solution and solid precipitates are present. To be clear, this exercise is intended to be a demonstration problem to demonstrate capabilities — not to accurately predict the MSRE, at least at this time. The temperature range was 300 °C (at no power) to 1500 °C at 7.25 MW, full power (thermal). The temperature and power are plotted in Fig. 3.

The original fuel/coolant mixture for the MSRE included zirconium, which cannot be used in the present example because it is not included in the current version of the MSTDB database [34]. Therefore, the fuel-loaded coolant was chosen to be stoichiometric FLiBe mixture with 10% UF_4 added. Specifically, the starting composition of this is example is a 2:1:0.1 mixture of LiF, BeF_2, and UF_4. In total, 10^5 moles of FLiBe (and 10^4 moles of UF_4) were input into ORIGEN-S as an initial fuel

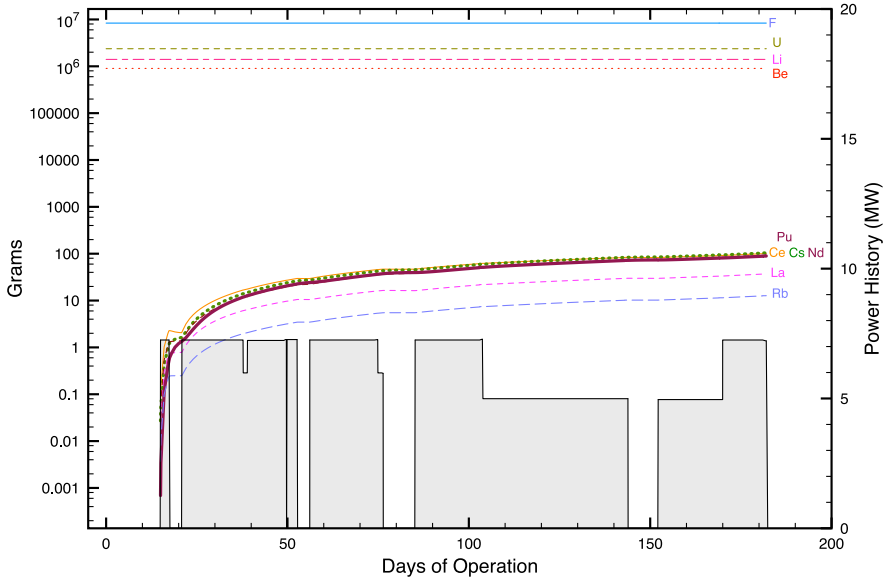

Fig. 4. Evolution of fuel mixture and fission product isotopes, as calculated by ORIGEN.

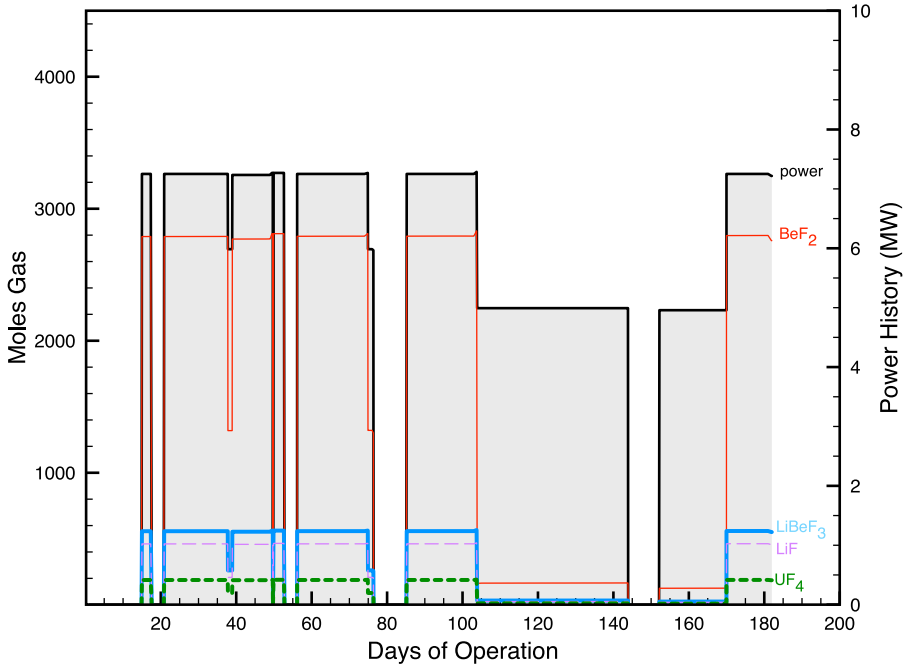

Fig. 5. Major ideal gas species, calculated by Thermochimica based on ORIGEN's isotopic evolution.

composition. At the time this manuscript was prepared, the MSTDB database [34] contains the elements Pu, U, Th, Nd, Ce, La, Cs, Rb, Ca, K, Na, F, Be, and Li. However, this example involves no Th fuel, and no Ca, K, or Na from the irradiation and decay calculation. Therefore, Pu, U, Nd, Ce, La, Cs, Rb, F, Be and Li were included in the solution.

Time stepping was daily for 182 days, except when there was a change in power during a day, in which case time stepping was more frequent. For cross-section interpolation, a library for a Westinghouse 17 × 17 assembly was used [42], as authentic molten salt reactor libraries were unavailable. The evolution of the fuel and fission product isotope concentrations is plotted in Fig. 4. Little change was seen in the fuel mixture isotopes, which was to be expected, while the fission and activation products built up gradually throughout the irradiation, with their levels plateauing whenever the MSRE was powered down. In particular, relatively large amounts of Pu, Ce, Cs, Nd, La and Rb were predicted to be generated.

These fission and activation products produced complex chemical solutions. While the pairs and quadruplets in the liquid solution phase (represented by the MQM) are too many to enumerate, the species in the ideal gas phase with the highest concentrations are plotted in Fig. 5. It can be seen that the quantities of the species involved

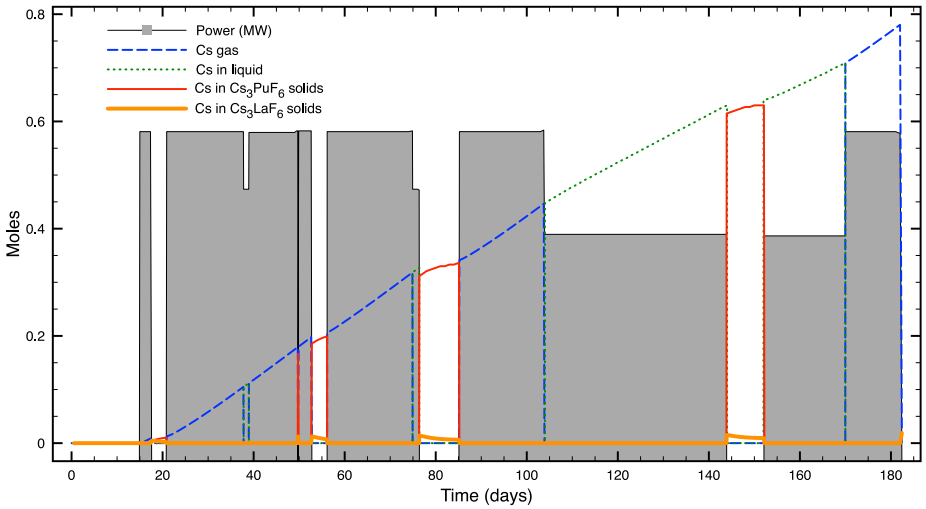

Fig. 6. Cs present is gas, liquid and solid phases. An important consideration for nuclear safety, as Cs is a radiotoxin.

strongly depends on the power, which controls the temperature in this simulation.

As a final illustration of the capability, the quantities of Cs found in gas, liquid and solid phases are plotted in Fig. 6. This information is important from a nuclear safety perspective, as Cs is a known volatile fission product and is radio-toxic if released. Again, it is worth emphasizing that this is a demonstration problem intended to demonstrate capabilities for continued investigation; one should not view the results as complete or completely representative of a real system.

6. Discussion

As previously mentioned, one of the primary drivers of implementing the MQMQA into Thermochimica is to be able to develop multi-physics capabilities whereby the output of Thermochimica will provide input to other codes. The current work on molten salts is principally influenced by MSRs. It is worth discussing possible applications and forms of coupling that may be of interest to industry and government stakeholders.

The output provided by Thermochimica and other GEM solvers includes the quantities of phases that are predicted to be stable at equilibrium, their composition (e.g., quadruplet fractions of a salt), and other thermodynamic parameters related to the system. Some thermodynamic parameters that may be of interest to other codes include heat capacity, enthalpy, and entropy of the system, the chemical potentials of the system components, and driving forces of metastable phases. One could conceivably use the calculated heat capacity and enthalpy values computed by Thermochimica as input to heat transfer calculations as material properties and source terms, respectively. Chemical potential terms could be used as input to solid-state diffusion calculations, which has been done to simulate oxygen transport in urania [27] and metallic U–Zr nuclear fuel [43]. Similarly, chemical potential terms could also be used to inform phase field calculations to simulate phase transformations [44,45]. Also, the composition of a liquid phase could be coupled with material property models of viscosity and density for use in momentum equations.

Some practical applications of coupling thermodynamics with other physical phenomena are worth considering, building on the demonstration problem presented in Section 5. In the context of MSR applications, some broad applications include corrosion, precipitation, off-gassing, and materials accountancy. Corrosion is generally a widespread concern in all engineering disciplines, but is particularly challenging in the context of MSRs as the better part of the periodic table is represented in the salt due to the nature of nuclear fission. Moreover, the behavior of minor impurities (e.g., oxygen) may have an important impact on reactor behavior, particularly corrosion. Precipitation of certain components in an MSR is expected, notably the noble metals [46,47]; however, there is the potential for precipitation of some components from the salt under abnormal conditions, such as under-cooling. Conversely, over-heating scenarios that may result in off-gassing is also of importance, particularly in handling volatile fission product species that may be released in an accident scenario. The simulation shown in Fig. 6 gives an example of how Thermochimica can predict the relative amount of cesium is in the gas compared to in the liquid phase. Lastly, materials accountancy is important in the context of non-proliferation and safeguards of MSRs, whereby the solubility of fissile components (i.e., U and Pu) require accurate accountancy.

Recently, Thermochimica has been coupled to the virtual environment for reactor applications (VERA) [48] to provide thermodynamic data calculated using MQMQA during a simulation of the molten salt reactor experiment [49]. In particular, Thermochimica predicted the concentrations of fission products in the gas phase. An off-gas removal system modeled in VERA demonstrated that reactivity could be slightly enhanced through the removal of xenon, illustrating the value of species fraction information for reactor design.

7. Conclusion

Improvements to the chemical thermodynamics library Thermochimica have enabled many applications to simulations of molten salts, including nuclear fuel salt systems with fission and activation products. These developments include extension of the applicability of the software to include molten salt systems in the form of the MQMQA, and reduction of the computational cost of equilibrium thermodynamic calculations in multi-physics settings. These developments make Thermochimica the first open-source and readily couplable thermochemistry library to support the MQMQA.

As demonstrated, multi-physics simulations of molten salt thermodynamic systems under irradiation and decay are now possible via coupling of Thermochimica to the isotopic evolution code ORIGEN to provide an understanding of the quantity of radio-toxic gases in a molten salt fuel loop. However, there are numerous potential applications for thermochemical calculations of molten salt systems. These include calculations of fission gas release in molten salt reactors, corrosion reactions with salt loop components, and plating out of precipitates from molten salts.

Implementation of MQMQA in Thermochimica required explicit expressions for chemical potentials of the second-nearest-neighbor quadruplets for the purposes of Gibbs energy minimization. These derivations have been provided to assist researchers in developing new thermodynamic equilibrium solvers and in integrating the modified quasi-chemical model into their software.

Declaration of competing interest

The authors declare that they have no known competing financial interests or personal relationships that could have appeared to influence the work reported in this paper.

Acknowledgments

The authors thank O. Beneš (JRC) and T.M. Besmann (UofSC) for technical discussions. This research was funded, in part, by the U.S. Department of Energy Nuclear Energy Advanced Modeling and Simulation program. This research was undertaken, in part, thanks to funding from the Canada Research Chairs program and the Discovery Grant Program of the Natural Sciences and Engineering Research Council of Canada.

Appendix A

A.1. Extended derivations

Some steps omitted from the derivations in the main text are included below for curious readers.

Eq. (34):

$$
\begin{aligned}
\frac{\partial(\Delta g_{ij/kk,\alpha})}{\partial n_{ab/xy}} &= g_{ij/kk,\alpha}\frac{\partial}{\partial n_{ab/xy}}\left[\chi_{ij/kk}^{p_\alpha}\chi_{ji/kk}^{q_\alpha}\right]\\
&= g_{ij/kk,\alpha}\frac{\partial}{\partial n_{ab/xy}}\left[\left(\frac{\sum_{c=\{i,\nu\}}\sum_{d=\{i,\nu\}}X_{cd/kk}}{\sum_{c=\{i,j,\nu,\gamma\}}\sum_{d=\{i,j,\nu,\gamma\}}X_{cd/kk}}\right)^{p_\alpha}\right.\\
&\quad\left.\times\left(\frac{\sum_{c=\{j,\gamma\}}\sum_{d=\{j,\gamma\}}X_{cd/kk}}{\sum_{c=\{i,j,\nu,\gamma\}}\sum_{d=\{i,j,\nu,\gamma\}}X_{cd/kk}}\right)^{q_\alpha}\right]\\
&= g_{ij/kk,\alpha}\frac{\partial}{\partial n_{ab/xy}}\left[\frac{\left(\sum_{c=\{i,\nu\}}\sum_{d=\{i,\nu\}}n_{cd/kk}\right)^{p_\alpha}\left(\sum_{c=\{j,\gamma\}}\sum_{d=\{j,\gamma\}}n_{cd/kk}\right)^{q_\alpha}}{\left(\sum_{c=\{i,j,\nu,\gamma\}}\sum_{d=\{i,j,\nu,\gamma\}}n_{cd/kk}\right)^{p_\alpha+q_\alpha}}\right]\\
&= g_{ij/kk,\alpha}\delta_{xk}\delta_{yk}\left[\frac{\left(\sum_{e=i,\nu}\delta_{ae}\right)\left(\sum_{e=i,\nu}\delta_{be}\right)p_\alpha}{\sum_{c=\{i,\nu\}}\sum_{d=\{i,\nu\}}n_{cd/kk}}+\frac{\left(\sum_{e=j,\gamma}\delta_{ae}\right)\left(\sum_{e=j,\gamma}\delta_{be}\right)q_\alpha}{\sum_{c=\{j,\gamma\}}\sum_{d=\{j,\gamma\}}n_{cd/kk}}\right.\\
&\quad\left.-\frac{\left(\sum_{e=i,\nu}\delta_{ae}+\sum_{e=j,\gamma}\delta_{ae}\right)\left(\sum_{e=i,\nu}\delta_{be}+\sum_{e=j,\gamma}\delta_{be}\right)(p_\alpha+q_\alpha)}{\sum_{c=\{i,j,\nu,\gamma\}}\sum_{d=\{i,j,\nu,\gamma\}}n_{cd/kk}}\right]\\
&\quad\cdot\left[\frac{\left(\sum_{c=\{i,\nu\}}\sum_{d=\{i,\nu\}}n_{cd/kk}\right)^{p_\alpha}\left(\sum_{c=\{j,\gamma\}}\sum_{d=\{j,\gamma\}}n_{cd/kk}\right)^{q_\alpha}}{\left(\sum_{c=\{i,j,\nu,\gamma\}}\sum_{d=\{i,j,\nu,\gamma\}}n_{cd/kk}\right)^{p_\alpha+q_\alpha}}\right] \qquad \text{(A.1)}\\
&= \Delta g_{ij/kk,\alpha}\frac{\delta_{xk}\delta_{yk}}{\sum_{c=\{i,j,\nu,\gamma\}}\sum_{d=\{i,j,\nu,\gamma\}}n_{cd/kk}}\left[\frac{\left(\sum_{e=i,\nu}\delta_{ae}\right)\left(\sum_{e=i,\nu}\delta_{be}\right)p_\alpha}{\chi_{ij/kk}}\right.\\
&\quad+\frac{\left(\sum_{e=j,\gamma}\delta_{ae}\right)\left(\sum_{e=j,\gamma}\delta_{be}\right)q_\alpha}{\chi_{ji/kk}}-\left(\sum_{e=i,\nu}\delta_{ae}+\sum_{e=j,\gamma}\delta_{ae}\right)\\
&\quad\left.\times\left(\sum_{e=i,\nu}\delta_{be}+\sum_{e=j,\gamma}\delta_{be}\right)(p_\alpha+q_\alpha)\right]\\
&= \frac{\Delta g_{ij/kk,\alpha}}{\sum_{cd/vw}n_{cd/vw}}\cdot\frac{\delta_{xk}\delta_{yk}}{\sum_{c=\{i,j,\nu,\gamma\}}\sum_{d=\{i,j,\nu,\gamma\}}X_{cd/kk}}\left[\frac{\left(\sum_{e=i,\nu}\delta_{ae}\right)\left(\sum_{e=i,\nu}\delta_{be}\right)p_\alpha}{\chi_{ij/kk}}\right.\\
&\quad+\frac{\left(\sum_{e=j,\gamma}\delta_{ae}\right)\left(\sum_{e=j,\gamma}\delta_{be}\right)q_\alpha}{\chi_{ji/kk}}-\left(\sum_{e=i,\nu}\delta_{ae}+\sum_{e=j,\gamma}\delta_{ae}\right)\\
&\quad\left.\times\left(\sum_{e=i,\nu}\delta_{be}+\sum_{e=j,\gamma}\delta_{be}\right)(p_\alpha+q_\alpha)\right].
\end{aligned}
$$

Eq. (35) is given in Box III.

Eq. (36) is given in Box IV.

Eq. (38):

$$
\begin{aligned}
&\frac{\partial}{\partial n_{ab/xy}}\left[Y_{m/k}\left(1-\xi_{ij/k}-\xi_{ji/k}\right)^{r_\alpha-1}\right]\\
&= \frac{\partial}{\partial n_{ab/xy}}\left[Y_{m/k}\left(1-\sum_{e=\{i,\nu\}}Y_{e/k}-\sum_{e=\{j,\gamma\}}Y_{e/k}\right)^{r_\alpha-1}\right]\\
&= \frac{\partial}{\partial n_{ab/xy}}\left[\left(\sum_{cd/vw}X_{cd/vw}\left(\frac{(\delta_{cm}+\delta_{dm})(\delta_{vk}+\delta_{wk})}{4}\right)\right)\right.\\
&\quad\left\{1-\left(\sum_{e=\{i,\nu\}}\sum_{cd/vw}X_{cd/vw}\left(\frac{(\delta_{ce}+\delta_{de})(\delta_{vk}+\delta_{wk})}{4}\right)\right)\right.\\
&\quad\left.\left.-\left(\sum_{e=\{j,\gamma\}}\sum_{cd/vw}X_{cd/vw}\left(\frac{(\delta_{ce}+\delta_{de})(\delta_{vk}+\delta_{wk})}{4}\right)\right)\right\}^{r_\alpha-1}\right]\\
&= \frac{\partial}{\partial n_{ab/xy}}\left[\left(\frac{1}{\sum_{cd/vw}n_{cd/vw}}\right)^{r_\alpha}\left(\sum_{cd/vw}n_{cd/vw}\left(\frac{(\delta_{cm}+\delta_{dm})(\delta_{vk}+\delta_{wk})}{4}\right)\right)\right.\\
&\quad\left\{\sum_{cd/vw}n_{cd/vw}-\left(\sum_{e=\{i,\nu\}}\sum_{cd/vw}n_{cd/vw}\left(\frac{(\delta_{ce}+\delta_{de})(\delta_{vk}+\delta_{wk})}{4}\right)\right)\right.\\
&\quad\left.\left.-\left(\sum_{e=\{j,\gamma\}}\sum_{cd/vw}n_{cd/vw}\left(\frac{(\delta_{ce}+\delta_{de})(\delta_{vk}+\delta_{wk})}{4}\right)\right)\right\}^{r_\alpha-1}\right]\\
&= \left(\frac{Y_{m/k}\left(1-\xi_{ij/k}-\xi_{ji/k}\right)^{r_\alpha-1}}{\sum_{cd/vw}n_{cd/vw}}\right)\\
&\quad\cdot\left[-(r_\alpha)+\left(\frac{(\delta_{am}+\delta_{bm})(\delta_{xk}+\delta_{yk})}{4}\right)\left(\frac{1}{Y_{m/k}}\right)\right.\\
&\quad+(r_\alpha-1)\left\{1-\xi_{ij}-\xi_{ji}\right\}^{-1}\\
&\quad\cdot\left\{1-\sum_{e=\{i,\nu\}}\left(\frac{(\delta_{ae}+\delta_{be})(\delta_{xk}+\delta_{yk})}{4}\right)\right.\\
&\quad\left.\left.-\sum_{e=\{j,\gamma\}}\left(\frac{(\delta_{ae}+\delta_{be})(\delta_{xk}+\delta_{yk})}{4}\right)\right\}\right]
\end{aligned}
\qquad \text{(A.4)}
$$

A.2. Thermochimica – FactSage comparison data

See Tables A.3 and A.4.

Appendix B. Supplementary data

Supplementary material related to this article can be found online at https://doi.org/10.1016/j.calphad.2021.102341.

$$
\begin{aligned}
\frac{\partial(\Delta g_{ij/kk,a})}{\partial n_{ab/xy}} &= g_{ij/kk,a}\frac{\partial}{\partial n_{ab/xy}}\left[\frac{\xi_{ij/k}^{p_a}\xi_{ji/k}^{q_a}}{(\xi_{ij/k}+\xi_{ji/k})^{p_a+q_a}}\right] \\
&= g_{ij/kk,a}\frac{\partial}{\partial n_{ab/xy}}\left[\frac{\left(\sum_{e=\{i,v\}}Y_{e/k}\right)^{p_a}\left(\sum_{e=\{j,\gamma\}}Y_{e/k}\right)^{q_a}}{\left(\sum_{e=\{i,v\}}Y_{e/k}+\sum_{e=\{j,\gamma\}}Y_{e/k}\right)^{p_a+q_a}}\right] \\
&= g_{ij/kk,a}\frac{\partial}{\partial n_{ab/xy}}\left[\left(\sum_{e=\{i,v\}}\sum_{cd/vw}X_{cd/vw}\left(\frac{(\delta_{ce}+\delta_{de})(\delta_{vk}+\delta_{wk})}{4}\right)\right)^{p_a}\cdot\left(\sum_{e=\{j,\gamma\}}\sum_{cd/vw}X_{cd/vw}\left(\frac{(\delta_{ce}+\delta_{de})(\delta_{vk}+\delta_{wk})}{4}\right)\right)^{q_a}\right. \\
&\qquad\left.\Big/\left(\sum_{e=\{i,v\}}\sum_{cd/vw}X_{cd/vw}\left(\frac{(\delta_{ce}+\delta_{de})(\delta_{vk}+\delta_{wk})}{4}\right)+\sum_{e=\{j,\gamma\}}\sum_{cd/vw}X_{cd/vw}\left(\frac{(\delta_{ce}+\delta_{de})(\delta_{vk}+\delta_{wk})}{4}\right)\right)^{p_a+q_a}\right] \\
&= g_{ij/kk,a}\frac{\partial}{\partial n_{ab/xy}}\left[\left(\sum_{e=\{i,v\}}\sum_{cd/vw}n_{cd/vw}\left(\frac{(\delta_{ce}+\delta_{de})(\delta_{vk}+\delta_{wk})}{4}\right)\right)^{p_a}\cdot\left(\sum_{e=\{j,\gamma\}}\sum_{cd/vw}n_{cd/vw}\left(\frac{(\delta_{ce}+\delta_{de})(\delta_{vk}+\delta_{wk})}{4}\right)\right)^{q_a}\right. \\
&\qquad\left.\Big/\left(\sum_{e=\{i,v\}}\sum_{cd/vw}n_{cd/vw}\left(\frac{(\delta_{ce}+\delta_{de})(\delta_{vk}+\delta_{wk})}{4}\right)+\sum_{e=\{j,\gamma\}}\sum_{cd/vw}n_{cd/vw}\left(\frac{(\delta_{ce}+\delta_{de})(\delta_{vk}+\delta_{wk})}{4}\right)\right)^{p_a+q_a}\right] \\
&= \Delta g_{ij/kk,a}\left[\left(\sum_{e=\{i,v\}}\frac{(\delta_{ae}+\delta_{be})(\delta_{xk}+\delta_{yk})}{4}\right)\left(\frac{p_\alpha}{\sum_{e=\{i,v\}}\sum_{cd/vw}n_{cd/vw}\left(\frac{(\delta_{ce}+\delta_{de})(\delta_{vk}+\delta_{wk})}{4}\right)}-\frac{p_\alpha+q_\alpha}{\sum_{e=\{i,v\}}\sum_{cd/vw}n_{cd/vw}\left(\frac{(\delta_{ce}+\delta_{de})(\delta_{vk}+\delta_{wk})}{4}\right)+\sum_{e=\{j,\gamma\}}\sum_{cd/vw}n_{cd/vw}\left(\frac{(\delta_{ce}+\delta_{de})(\delta_{ik}+\delta_{wk})}{4}\right)}\right)\right. \\
&\qquad\left.+\left(\sum_{e=\{j,\gamma\}}\frac{(\delta_{ae}+\delta_{be})(\delta_{xk}+\delta_{yk})}{4}\right)\left(\frac{q_\alpha}{\sum_{e=\{j,\gamma\}}\sum_{cd/vw}n_{cd/vw}\left(\frac{(\delta_{ce}+\delta_{de})(\delta_{vk}+\delta_{wk})}{4}\right)}-\frac{p_\alpha+q_\alpha}{\sum_{e=\{i,v\}}\sum_{cd/vw}n_{cd/vw}\left(\frac{(\delta_{ce}+\delta_{de})(\delta_{vk}+\delta_{wk})}{4}\right)+\sum_{e=\{j,\gamma\}}\sum_{cd/vw}n_{cd/vw}\left(\frac{(\delta_{ce}+\delta_{de})(\delta_{ik}+\delta_{wk})}{4}\right)}\right)\right] \\
&= \frac{\Delta g_{ij/kk,a}}{\sum_{cd/vw}n_{cd/vw}}\left[\left(\sum_{e=\{i,v\}}\frac{(\delta_{ae}+\delta_{be})(\delta_{xk}+\delta_{yk})}{4}\right)\left(\frac{p_\alpha}{\xi_{ij/k}}-\frac{p_\alpha+q_\alpha}{\xi_{ij/k}+\xi_{ji/k}}\right)+\left(\sum_{e=\{j,\gamma\}}\frac{(\delta_{ae}+\delta_{be})(\delta_{xk}+\delta_{yk})}{4}\right)\left(\frac{q_\alpha}{\xi_{ji/k}}-\frac{p_\alpha+q_\alpha}{\xi_{ij/k}+\xi_{ji/k}}\right)\right],
\end{aligned}
\tag{A.2}
$$

Box III.

$$
\begin{aligned}
&\frac{\partial}{\partial n_{ab/xy}}\left[\left(\frac{Y_{m/k}}{\xi_{ji/k}}\right)\left(1-\frac{Y_{j/k}}{\xi_{ji/k}}\right)^{r_\alpha-1}\right]=\frac{\partial}{\partial n_{ab/xy}}\left[\left(\frac{Y_{m/k}}{\sum_{e=\{j,\gamma\}}Y_{e/k}}\right)\left(1-\frac{Y_{j/k}}{\sum_{e=\{j,\gamma\}}Y_{e/k}}\right)^{r_\alpha-1}\right] \\
&=\frac{\partial}{\partial n_{ab/xy}}\left[\left(\frac{\sum_{cd/vw}X_{cd/vw}\left(\frac{(\delta_{cm}+\delta_{dm})(\delta_{vk}+\delta_{wk})}{4}\right)}{\sum_{e=\{j,\gamma\}}\sum_{cd/vw}X_{cd/vw}\left(\frac{(\delta_{ce}+\delta_{de})(\delta_{vk}+\delta_{wk})}{4}\right)}\right)\cdot\left(1-\frac{\sum_{cd/vw}X_{cd/vw}\left(\frac{(\delta_{cj}+\delta_{dj})(\delta_{vk}+\delta_{wk})}{4}\right)}{\sum_{e=\{j,\gamma\}}\sum_{cd/vw}X_{cd/vw}\left(\frac{(\delta_{ce}+\delta_{de})(\delta_{vk}+\delta_{wk})}{4}\right)}\right)^{r_\alpha-1}\right] \\
&=\frac{\partial}{\partial n_{ab/xy}}\left[\left(\frac{\sum_{cd/vw}n_{cd/vw}\left(\frac{(\delta_{cm}+\delta_{dm})(\delta_{vk}+\delta_{wk})}{4}\right)}{\sum_{e=\{j,\gamma\}}\sum_{cd/vw}n_{cd/vw}\left(\frac{(\delta_{ce}+\delta_{de})(\delta_{vk}+\delta_{wk})}{4}\right)}\right)\cdot\left(1-\frac{\sum_{cd/vw}n_{cd/vw}\left(\frac{(\delta_{cj}+\delta_{dj})(\delta_{vk}+\delta_{wk})}{4}\right)}{\sum_{e=\{j,\gamma\}}\sum_{cd/vw}n_{cd/vw}\left(\frac{(\delta_{ce}+\delta_{de})(\delta_{vk}+\delta_{wk})}{4}\right)}\right)^{r_\alpha-1}\right] \\
&=\left(\frac{Y_{m/k}}{\xi_{ji/k}}\right)\left(1-\frac{Y_{j/k}}{\xi_{ji/k}}\right)^{r_\alpha-1}\left[\left(\frac{\frac{(\delta_{am}+\delta_{bm})(\delta_{xk}+\delta_{yk})}{4}}{\sum_{cd/vw}n_{cd/vw}\left(\frac{(\delta_{cm}+\delta_{dm})(\delta_{vk}+\delta_{wk})}{4}\right)}\right)-\left(\frac{\sum_{e=\{j,\gamma\}}\frac{(\delta_{ae}+\delta_{be})(\delta_{xk}+\delta_{yk})}{4}}{\sum_{e=\{j,\gamma\}}\sum_{cd/vw}n_{cd/vw}\left(\frac{(\delta_{ce}+\delta_{de})(\delta_{vk}+\delta_{wk})}{4}\right)}\right)-\left(\frac{r_\alpha-1}{\sum_{e=\{j,\gamma\}}\sum_{cd/vw}n_{cd/vw}\left(\frac{(\delta_{ce}+\delta_{de})(\delta_{vk}+\delta_{wk})}{4}\right)}\right)\right. \\
&\qquad\left.\cdot\left(1-\frac{\sum_{cd/vw}n_{cd/vw}\left(\frac{(\delta_{cj}+\delta_{dj})(\delta_{vk}+\delta_{wk})}{4}\right)}{\sum_{e=\{j,\gamma\}}\sum_{cd/vw}n_{cd/vw}\left(\frac{(\delta_{ce}+\delta_{de})(\delta_{ik}+\delta_{wk})}{4}\right)}\right)^{-1}\times\left\{\left(\frac{(\delta_{aj}+\delta_{bj})(\delta_{xk}+\delta_{yk})}{4}\right)-\left(\sum_{cd/vw}n_{cd/vw}\left(\frac{(\delta_{cj}+\delta_{dj})(\delta_{vk}+\delta_{wk})}{4}\right)\right)\cdot\left(\frac{\sum_{e=\{j,\gamma\}}\frac{(\delta_{ae}+\delta_{be})(\delta_{xk}+\delta_{yk})}{4}}{\sum_{e=\{j,\gamma\}}\sum_{cd/vw}n_{cd/vw}\left(\frac{(\delta_{ce}+\delta_{de})(\delta_{vk}+\delta_{wk})}{4}\right)}\right)\right\}\right] \\
&=\left(\frac{1}{\sum_{cd/vw}n_{cd/vw}}\right)\left(\frac{Y_{m/k}}{\xi_{ji/k}}\right)\left(1-\frac{Y_{j/k}}{\xi_{ji/k}}\right)^{r_\alpha-1}\times\left[\left(\frac{(\delta_{am}+\delta_{bm})(\delta_{xk}+\delta_{yk})}{4Y_{m/k}}\right)-\left(\sum_{e=\{j,\gamma\}}\frac{(\delta_{ae}+\delta_{be})(\delta_{xk}+\delta_{yk})}{4\xi_{ji/k}}\right)\right. \\
&\qquad\left.-\left(\frac{r_\alpha-1}{\xi_{ji/k}}\right)\left(1-\frac{Y_{j/k}}{\xi_{ji/k}}\right)^{-1}\left\{\left(\frac{(\delta_{aj}+\delta_{bj})(\delta_{xk}+\delta_{yk})}{4}\right)-Y_{j/k}\left(\sum_{e=\{j,\gamma\}}\frac{(\delta_{ae}+\delta_{be})(\delta_{xk}+\delta_{yk})}{4\xi_{ji/k}}\right)\right\}\right]
\end{aligned}
\tag{A.3}
$$

Box IV.

Table A.3
Output species concentrations from Thermochimica and FactSage for a nuclear fuel salt mixture with composition given in Table 1 at 1500 K and 1 atm. Both codes predict the only stable phase to be the MQMQA liquid phase, and report integral Gibbs energies of −2.97876E+11 J.

Quadruplet	Thermochimica concentration	FactSage concentration	Quadruplet	Thermochimica concentration	FactSage concentration
Li-Li-F-F	2.2900E−01	2.2900E−01	Be-Be-F-F	1.0924E−01	1.0924E−01
U4+-U4+-F-F	1.2628E−03	1.2628E−03	U3+-U3+-F-F	1.5049E−04	1.5049E−04
Pu-Pu-F-F	1.3270E−12	1.3270E−12	Rb-Rb-F-F	1.5842E−13	1.5842E−13
La-La-F-F	6.5030E−13	6.5030E−13	Cs-Cs-F-F	4.1464E−12	4.1464E−12
Ce-Ce-F-F	4.6936E−12	4.6936E−12	Nd-Nd-F-F	3.4270E−12	3.4270E−12
Li-Be-F-F	5.7574E−01	5.7574E−01	Li-U4+-F-F	5.2667E−02	5.2667E−02
Be-U4+-F-F	1.4110E−02	1.4110E−02	Li-U3+-F-F	8.6840E−03	8.6840E−03
Be-U3+-F-F	8.1004E−03	8.1004E−03	U4+-U3+-F-F	1.0293E−03	1.0293E−03
Li-Pu-F-F	9.3913E−07	9.3913E−07	Be-Pu-F-F	7.1114E−07	7.1114E−07
U4+-Pu-F-F	7.6367E−08	7.6367E−08	U3+-Pu-F-F	2.8211E−08	2.8211E−08
Li-Rb-F-F	4.5935E−07	4.5935E−07	Be-Rb-F-F	2.3392E−07	2.3392E−07
U4+-Rb-F-F	2.5197E−08	2.5197E−08	U3+-Rb-F-F	8.6594E−09	8.6594E−09
Pu-Rb-F-F	2.6577E−12	2.6577E−12	Li-La-F-F	7.1228E−07	7.1228E−07
Be-La-F-F	5.3347E−07	5.3347E−07	U4+-La-F-F	5.7465E−08	5.7465E−08
U3+-La-F-F	1.9749E−08	1.9749E−08	Pu-La-F-F	1.8579E−12	1.8579E−12
Rb-La-F-F	1.8000E−12	1.8000E−12	Li-Cs-F-F	2.3851E−06	2.3851E−06
Be-Cs-F-F	1.1967E−06	1.1967E−06	U4+-Cs-F-F	1.2891E−07	1.2891E−07
U3+-Cs-F-F	4.4302E−08	4.4302E−08	Pu-Cs-F-F	1.1261E−11	1.1261E−11
Rb-Cs-F-F	1.6209E−12	1.6209E−12	La-Cs-F-F	8.1914E−12	8.1913E−12
Li-Ce-F-F	2.0397E−06	2.0397E−06	Be-Ce-F-F	1.4332E−06	1.4332E−06
U4+-Ce-F-F	2.0742E−07	2.0742E−07	U3+-Ce-F-F	5.3056E−08	5.3056E−08
Pu-Ce-F-F	4.9913E−12	4.9913E−12	Rb-Ce-F-F	1.5321E−12	1.5321E−12
La-Ce-F-F	3.4942E−12	3.4941E−12	Cs-Ce-F-F	7.8384E−12	7.8384E−12
Li-Nd-F-F	1.5296E−06	1.5296E−06	Be-Nd-F-F	1.2246E−06	1.2246E−06
U4+-Nd-F-F	1.7724E−07	1.7724E−07	U3+-Nd-F-F	4.5336E−08	4.5335E−08
Pu-Nd-F-F	4.2650E−12	4.2650E−12	Rb-Nd-F-F	1.3092E−12	1.3092E−12
La-Nd-F-F	2.9857E−12	2.9857E−12	Cs-Nd-F-F	6.6978E−12	6.6978E−12
Ce-Nd-F-F	8.0213E−12	8.0212E−12			

Table A.4
Output species concentrations from Thermochimica and FactSage for a nuclear fuel salt mixture with composition given in Table 2 at 1500 K and 1 atm. Both codes predict the only stable phase to be the MQMQA liquid phase, and report integral Gibbs energies of −3.68872E+11 J.

Quadruplet	Thermochimica concentration	FactSage concentration	Quadruplet	Thermochimica concentration	FactSage concentration
Na-Na-Cl-Cl	1.0005E−01	1.0005E−01	Mg-Mg-Cl-Cl	4.4044E−03	4.4044E−03
U-U-Cl-Cl	3.1325E−12	3.1331E−12	Pu-Pu-Cl-Cl	1.9104E−07	1.9105E−07
Cs-Cs-Cl-Cl	3.5647E−07	3.5647E−07	K-K-Cl-Cl	8.2765E−02	8.2765E−02
Li-Li-Cl-Cl	3.3919E−02	3.3919E−02	Na-Mg-Cl-Cl	6.4751E−02	6.4751E−02
Na-U-Cl-Cl	3.3910E−05	3.3912E−05	Mg-U-Cl-Cl	5.5774E−07	5.5778E−07
Na-Pu-Cl-Cl	4.3942E−04	4.3943E−04	Mg-Pu-Cl-Cl	4.0678E−05	4.0679E−05
U-Pu-Cl-Cl	1.0024E−10	1.0025E−10	Na-Cs-Cl-Cl	4.1226E−04	4.1226E−04
Mg-Cs-Cl-Cl	1.8007E−04	1.8007E−04	U-Cs-Cl-Cl	4.2221E−08	4.2223E−08
Pu-Cs-Cl-Cl	5.1617E−07	5.1618E−07	Na-K-Cl-Cl	1.8339E−01	1.8339E−01
Mg-K-Cl-Cl	7.5215E−02	7.5215E−02	U-K-Cl-Cl	2.3603E−05	2.3604E−05
Pu-K-Cl-Cl	2.5055E−04	2.5055E−04	Cs-K-Cl-Cl	3.4626E−04	3.4626E−04
Na-Li-Cl-Cl	1.1484E−01	1.1484E−01	Mg-Li-Cl-Cl	2.3845E−02	2.3845E−02
U-Li-Cl-Cl	1.7332E−05	1.7333E−05	Pu-Li-Cl-Cl	1.5690E−04	1.5690E−04
Cs-Li-Cl-Cl	2.1684E−04	2.1684E−04	K-Li-Cl-Cl	1.2074E−01	1.2074E−01
Na-Na-Va-Va	1.4810E−04	1.4811E−04	Mg-Mg-Va-Va	2.5668E−02	2.5667E−02
U-U-Va-Va	8.1970E−04	8.1970E−04	Pu-Pu-Va-Va	8.4302E−05	8.4300E−05
Cs-Cs-Va-Va	4.8365E−11	4.8367E−11	K-K-Va-Va	2.2672E−04	2.2672E−04
Li-Li-Va-Va	1.2612E−05	1.2612E−05	Na-Mg-Va-Va	3.8995E−03	3.8995E−03
Na-U-Va-Va	6.9685E−04	6.9686E−04	Mg-U-Va-Va	9.1738E−03	9.1738E−03
Na-Pu-Va-Va	2.2348E−04	2.2348E−04	Mg-Pu-Va-Va	2.9420E−03	2.9419E−03
U-Pu-Va-Va	5.2575E−04	5.2574E−04	Na-Cs-Va-Va	1.6927E−07	1.6927E−07
Mg-Cs-Va-Va	2.2284E−06	2.2284E−06	U-Cs-Va-Va	3.9822E−07	3.9823E−07
Pu-Cs-Va-Va	1.2771E−07	1.2771E−07	Na-K-Va-Va	3.6648E−04	3.6649E−04
Mg-K-Va-Va	4.8246E−03	4.8246E−03	U-K-Va-Va	8.6218E−04	8.6219E−04
Pu-K-Va-Va	2.7650E−04	2.7650E−04	Cs-K-Va-Va	2.0943E−07	2.0943E−07
Na-Li-Va-Va	8.6437E−05	8.6440E−05	Mg-Li-Va-Va	1.1379E−03	1.1379E−03
U-Li-Va-Va	2.0335E−04	2.0335E−04	Pu-Li-Va-Va	6.5213E−05	6.5214E−05
Cs-Li-Va-Va	4.9395E−08	4.9397E−08	K-Li-Va-Va	1.0694E−04	1.0695E−04
Na-Na-Cl-Va	7.7076E−03	7.7077E−03	Mg-Mg-Cl-Va	2.0854E−02	2.0854E−02
U-U-Cl-Va	2.0058E−06	2.0059E−06	Pu-Pu-Cl-Va	7.8640E−06	7.8641E−06
Cs-Cs-Cl-Va	8.3164E−09	8.3166E−09	K-K-Cl-Va	8.7400E−03	8.7401E−03
Li-Li-Cl-Va	1.2909E−03	1.2909E−03	Na-Mg-Cl-Va	2.8148E−02	2.8148E−02
Na-U-Cl-Va	2.7715E−04	2.7716E−04	Mg-U-Cl-Va	3.4872E−04	3.4873E−04
Na-Pu-Cl-Va	5.5231E−04	5.5231E−04	Mg-Pu-Cl-Va	7.8157E−04	7.8157E−04
U-Pu-Cl-Va	9.1598E−06	9.1601E−06	Na-Cs-Cl-Va	1.6731E−05	1.6732E−05
Mg-Cs-Cl-Va	3.1949E−05	3.1950E−05	U-Cs-Cl-Va	2.5831E−07	2.5832E−07
Pu-Cs-Cl-Va	5.1147E−07	5.1148E−07	Na-K-Cl-Va	1.6415E−02	1.6415E−02

(*continued on next page*)

Table A.4 (*continued*).

Quadruplet	Thermochimica concentration	FactSage concentration	Quadruplet	Thermochimica concentration	FactSage concentration
Mg-K-Cl-Va	3.1444E−02	3.1444E−02	U-K-Cl-Va	2.4903E−04	2.4904E−04
Pu-K-Cl-Va	5.243E−04	5.2434E−04	Cs-K-Cl-Va	1.7051E−05	1.7051E−05
Na-Li-Cl-Va	6.3086E−03	6.3087E−03	Mg-Li-Cl-Va	1.0377E−02	1.0377E−02
U-Li-Cl-Va	1.1025E−04	1.1026E−04	Pu-Li-Cl-Va	2.0151E−04	2.0151E−04
Cs-Li-Cl-Va	6.5530E−06	6.5531E−06	K-Li-Cl-Va	7.1867E−03	7.1868E−03

References

[1] J. Serp, M. Allibert, O. Beneš, S. Delpech, O. Feynberg, V. Ghetta, D. Heuer, D. Holcomb, V. Ignatiev, J.L. Kloosterman, L. Luzzi, E. Merle-Lucotte, J. Uhlíř, R. Yoshioka, D. Zhimin, The molten salt reactor (MSR) in generation IV: overview and perspectives, Prog. Nucl. Energy 77 (2014) 308–319.

[2] A. Pelton, S. Degterov, G. Eriksson, C. Robelin, Y. Dessureault, The modified quasichemical model I – binary solutions, Metall. Mater. Trans. B 31B (2000) 651–659.

[3] A. Pelton, P. Chartrand, The modified quasichemical model II – multicomponent solutions, Metall. Mater. Trans. A 32A (2001) 1355–1360.

[4] P. Chartrand, A. Pelton, The modified quasichemical model III – two sublattices, Metall. Mater. Trans. A 32 (2001) 1397–1407.

[5] A. Pelton, P. Chartrand, G. Eriksson, The modified quasichemical model IV – two-sublattice quadruplet approximation, Metall. Mater. Trans. A 32 (2001) 1409–1416.

[6] G. Lambotte, P. Chartrand, Thermodynamic optimization of the (Na_2O + SiO_2 + NaF + SiF_4) reciprocal system using the modified quasichemical model in the quadruplet approximation, J. Chem. Thermodyn. 43 (2011) 1678–1699.

[7] P. Chartrand, A.D. Pelton, Thermodynamic evaluation and optimization of the LiF-NaF-KF-MgF_2-CaF_2 system using the modified quasi-chemical model, Metall. Mater. Trans. A 32 (6) (2001) 1385–1396.

[8] P. Chartrand, A.D. Pelton, Thermodynamic evaluation and optimization of the Li, Na, K, Mg, Ca//F, Cl reciprocal system using the modified quasi-chemical model, Metall. Mater. Trans. A 32 (6) (2001) 1417–1430.

[9] O. Beneš, J. Van der Meer, R. Konings, Modelling and calculation of the phase diagrams of the LiF–NaF–RbF–LaF_3 system, CALPHAD 31 (2) (2007) 209–216.

[10] M. Beilmann, O. Beneš, R. Konings, T. Fanghänel, Thermodynamic investigation of the (LiF+ NaF+ CaF_2+ LaF_3) system, J. Chem. Thermodyn. 43 (10) (2011) 1515–1524.

[11] O. Beneš, P. Souček, Molten salt reactor fuels, in: M.H. Piro (Ed.), Advances in Nuclear Fuel Chemistry, in: Woodhead Publishing Series in Energy, Woodhead Publishing, 2020, pp. 249–271.

[12] J. McMurray, T. Besmann, J. Ard, B. Fitzpatrick, M. Piro, J. Jerden, M. Williamson, B. Collins, B. Betzler, A. Qualls, Multi-Physics Simulations for Molten Salt Reactor Evaluation: Chemistry Modeling and Database Development, Tech. Rep. ORNL/SPR-2018/864, Oak Ridge National Laboratory, Oak Ridge, TN, 2018.

[13] K. Wang, Z. Fei, J. Wang, Z. Wu, C. Li, L. Xie, Thermodynamic description of the AgCl–$CoCl_2$–$InCl_3$–KCl system, Mater. Chem. Phys. 163 (2015) 73–87.

[14] J.W. McMurray, S.S. Raiman, Thermodynamic modeling of the K-KCl and Mg-$MgCl_2$ binary systems using the CALPHAD method, Sol. Energy 170 (2018) 1039–1042.

[15] C. Bale, P. Chartrand, S. Degterov, G. Eriksson, K. Hack, R. Mahfoud, J. Melançon, A. Pelton, S. Peterson, FactSage thermochemical software and databases, CALPHAD 26 (2) (2002).

[16] G. Lambotte, P. Chartrand, Thermodynamic evaluation and optimization of the Al_2O_3–SiO_2–AlF_3–SiF_4 reciprocal system using the modified quasichemical model, J. Am. Ceram. Soc. 94 (11) (2011) 4000–4008.

[17] G. Lambotte, P. Chartrand, Thermodynamic modeling of the (Al_2O_3+ Na_2O),(Al_2O_3+ Na_2O+ SiO_2), and (Al_2O3+ Na_2O+ AlF_3 + NaF) systems, J. Chem. Thermodyn. 57 (2013) 306–334.

[18] K. Wang, P. Chartrand, A thermodynamic description for water, hydrogen fluoride and hydrogen dissolutions in cryolite-base molten salts, Phys. Chem. Chem. Phys. 20 (25) (2018) 17324–17341.

[19] D. Shishin, E. Jak, S.A. Decterov, Thermodynamic assessment of slag–matte–metal equilibria in the Cu-Fe-OS-Si system, J. Phase Equilib. Diffus. 39 (5) (2018) 456–475.

[20] D. Shishin, T. Hidayat, J. Chen, P.C. Hayes, E. Jak, Combined experimental and thermodynamic modelling investigation of the distribution of antimony and tin between phases in the Cu-Fe-OS-Si system, CALPHAD 65 (2019) 16–24.

[21] D. Shishin, T. Hidayat, J. Chen, P.C. Hayes, E. Jak, Integrated experimental study and thermodynamic modelling of the distribution of arsenic between phases in the Cu-Fe-OS-Si system, J. Chem. Thermodyn. 135 (2019) 175–182.

[22] M. Piro, S. Simunovic, T. Besmann, B. Lewis, W. Thompson, The thermochemistry library THERMOCHIMICA, Comput. Mater. Sci. 67 (2013) 266–272.

[23] M. Piro, J. Banfield, K. Clarno, S. Simunovic, T. Besmann, B. Lewis, W. Thompson, Coupled thermochemical, isotopic evolution and heat transfer simulations in highly irradiated UO_2 nuclear fuel, J. Nucl. Mater. 441 (2013) 240–251.

[24] S. Simunovic, S.L. Voit, T.M. Besmann, Oxygen Diffusion Model using the Thermochimica Module in MOOSE/BISON, Tech. Rep. ORNL/TM-2014/293, Oak Ridge National Laboratory, Oak Ridge, TN (United States), 2014.

[25] S. Simunovic, T.M. Besmann, S.L. Voit, Benchmark Problem for Calculating Oxygen Potential in High Burnup LWR Fuel using the Thermochimica Module in MOOSE/BISON, Tech. Rep. ORNL/TM-2014/529, Oak Ridge National Laboratory, Oak Ridge, TN (United States), 2014.

[26] S. Simunovic, T.M. Besmann, Coupling of Thermochemistry Solver Thermochimica with MOOSE/BISON, Tech. Rep. ORNL/TM-2015/322, Oak Ridge National Laboratory, Oak Ridge, TN (United States), 2015, p. 25.

[27] S. Simunovic, T.M. Besmann, E. Moore, M. Poschmann, M.H. Piro, K.T. Clarno, J.W. McMurray, W.A. Wieselquist, Modeling and simulation of oxygen transport in high burnup LWR fuel, J. Nucl. Mater. (2020) 152194.

[28] M. Poschmann, M.H. Piro, T.M. Besmann, K.T. Clarno, S. Simunovic, Thermochemically-informed mass transport model for interdiffusion of U and Zr in irradiated U-Pu-Zr fuel with fission products, J. Nucl. Mater. 554 (2021) 153089.

[29] L.C. Olson, J.W. Ambrosek, K. Sridharan, M.H. Anderson, T.R. Allen, Materials corrosion in molten LiF–NaF–KF salt, J. Fluor. Chem. 130 (1) (2009) 67–73.

[30] W.B. White, S.M. Johnson, G.B. Dantzig, Chemical equilibrium in complex mixtures, J. Chem. Phys. 28 (5) (1958) 751–755.

[31] M.H.A. Piro, J. Banfield, K.T. Clarno, S. Simunovic, T.M. Besmann, B.J. Lewis, W.T. Thompson, Coupled thermochemical, isotopic evolution and heat transfer simulations in highly irradiated UO_2 nuclear fuel, J. Nucl. Mater. 441 (1–3) (2013) 240–251.

[32] M. Hillert, The compound energy formalism, J. Alloys Compd. 320 (2) (2001) 161–176.

[33] A.D. Pelton, Phase Diagrams and Thermodynamic Modeling of Solutions, Academic Press, 2018.

[34] T.M. Besmann, J. Ard, S. Utlak, J.W. McMurray, R.A. Lefebvre, Status of the Salt Thermochemical Database, Tech. Rep. ORNL/SPR-2019/1208, Oak Ridge National Laboratory, Oak Ridge, TN (United States), 2019.

[35] M.H.A. Piro, M. Poschmann, P. Bajpai, On the interpretation of chemical potentials computed from equilibrium thermodynamic codes: Applications to molten salts, J. Nucl. Mater. 526 (2019) 151756.

[36] G. Eriksson, W.T. Thompson, A procedure to estimate equilibrium concentrations in multicomponent systems amd related applications, CALPHAD 13 (4) (1989) 389–400.

[37] M. Piro, S. Simunovic, Performance enhancing algorithms for computing thermodynamic equilibria, CALPHAD 39 (2012) 104–110.

[38] M. Poschmann, M. Piro, S. Simunovic, Acceleration of Thermochimica Calculations in Bison, Report ORNL/TM-2020/1473, Oak Ridge National Laboratory, Oak Ridge, TN (United States), 2020.

[39] D. Gaston, C. Newman, G. Hansen, D. Lebrun-Grandie, MOOSE: A parallel computational framework for coupled systems of nonlinear equations, Nucl. Eng. Des. 239 (10) (2009) 1768–1778.

[40] M. Rosenthal, R. Briggs, P. Kasten, Molten Salt Reactor Program Semiannual Progress Report. For Period Ending February 29, 1968, Tech. Rep. ORNL-4254, Oak Ridge National Laboratory, Oak Ridge, TN (United States), 1968.

[41] O. Hermann, R. Westfall, ORIGEN-S: SCALE System Module to Calculate Fuel Depletion, Actinide Transmutation, Fission Product Buildup and Decay, and Associated Radiation Source Terms, Tech. Rep. ORNL/NUREG/CSD-2/V2/R6, Oak Ridge National Laboratory, 1998.

[42] M. Chadwick, M. Herman, P. Obložinský, M. Dunn, Y. Danon, A. Kahler, D. Smith, B. Pritychenko, G. Arbanas, R. Arcilla, R. Brewer, D. Brown, R. Capote, A. Carlson, Y. Cho, H. Derrien, K. Guber, G. Hale, S. Hoblit, S. Holloway, T. Johnson, T. Kawano, B. Kiedrowski, H. Kim, S. Kunieda, N. Larson, L. Leal, J. Lestone, R. Little, E. McCutchan, R. MacFarlane, M. MacInnes, C. Mattoon, R. McKnight, S. Mughabghab, G. Nobre, G. Palmiotti, A. Palumbo, M. Pigni, V. Pronyaev, R. Sayer, A. Sonzogni, N. Summers, P. Talou, I. Thompson, A. Trkov, R. Vogt, S. van der Marck, A. Wallner, M. White, D. Wiarda, P. Young, ENDF/B-VII.1 nuclear data for science and technology: Cross sections, covariances, fission product yields and decay data, Nucl. Data Sheets 112 (12) (2011) 2887–2996, Special Issue on ENDF/B-VII.1 Library.

[43] M. Poschmann, B.W. Fitzpatrick, S. Simunovic, M.H. Piro, Recent development of thermochimica for simulations of nuclear materials, in: TMS 2020 149th Annual Meeting & Exhibition Supplemental Proceedings, Springer, 2020, pp. 1003–1012.

[44] D. Schwen, L.K. Aagesen, J.W. Peterson, M.R. Tonks, Rapid multiphase-field model development using a modular free energy based approach with automatic differentiation in MOOSE/MARMOT, Comput. Mater. Sci. 132 (2017) 36–45.

[45] P. Bajpai, M. Poschmann, D. Andrš, C. Bhave, M. Tonks, M. Piro, Development of a new thermochemistry solver for multiphysics simulations of nuclear materials, in: TMS 2020 149th Annual Meeting & Exhibition Supplemental Proceedings, Springer International Publishing, Cham, 2020, pp. 1013–1025.

[46] D.J. Diamond, N.R. Brown, R. Denning, S. Bajorek, Phenomena Important in Molten Salt Reactor Simulations, Tech. Rep. BNL-114869-2017-INRE DE-SC0012704, Brookhaven National Lab.(BNL), Upton, NY (United States), 2018.

[47] J. McFarlane, P.A. Taylor, D.E. Holcomb, W. Poore III, Review of Hazards Associated with Molten Salt Reactor Fuel Processing Operations, Tech. Rep. ORNL/TM-2019/1195, Oak Ridge National Lab.(ORNL), Oak Ridge, TN (United States), 2019.

[48] J.A. Turner, K. Clarno, M. Sieger, R. Bartlett, B. Collins, R. Pawlowski, R. Schmidt, R. Summers, The virtual environment for reactor applications (VERA): design and architecture, J. Comput. Phys. 326 (2016) 544–568.

[49] A.M. Graham, Z. Taylor, B.S. Collins, R.K. Salko, M. Poschmann, Multiphysics coupling methods for molten salt reactor modeling and simulation in VERA, Nucl. Sci. Eng. (2021) 1–22.